UTAH GEOLOGICAL SURVEY
a division of
Utah Department of Natural Resources

Plate 1
Utah Geological Survey Miscellaneous Publication 175DM
Geologic Map of the Southern Half of the Rill Creek and Northern Half of the Kane Springs 7.5' Quadrangles

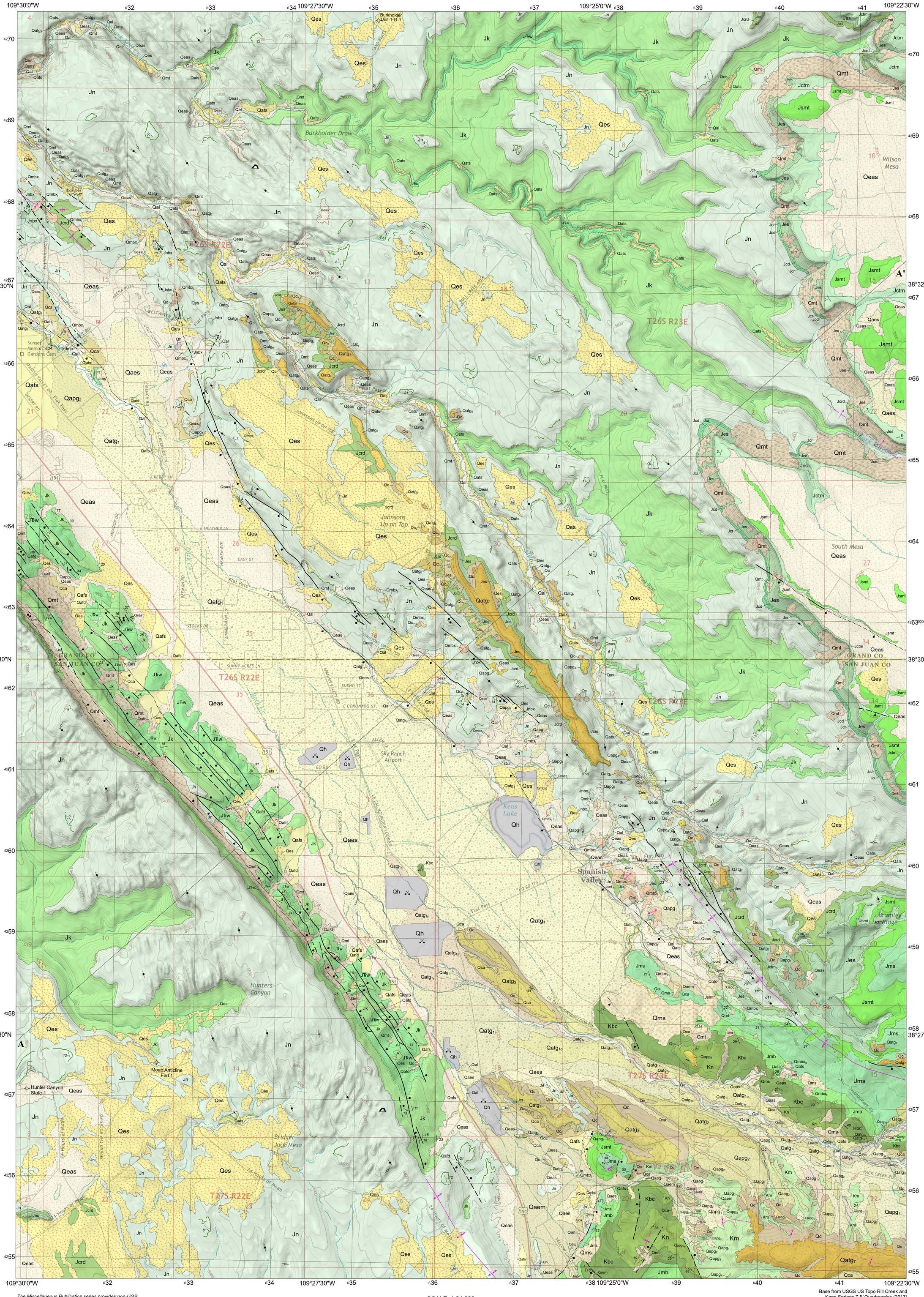

The Miscellaneous Publication series provides non-UGS authors with a high-quality format for documents concerning Utah geology. Although review comments have been incorporated, this document does not necessarily conform to UGS technical, editorial, or policy standards. The Utah Department of Natural Resources, Utah Geological Survey, makes no warranty, expressed or implied, regarding the suitability of this product for a particular use. The Utah Department of Natural Resources, Utah Geological Survey, shall not be liable under any circumstances for any direct, indirect, special, incidental, or consequential damages with respect to claims by users of this product. For use at 1:24,000 scale.

This geologic map was partially funded by the U.S. Geological Survey, National Cooperative Geologic Mapping Program, through USGS EDMAP agreement number G16AC00205 (2016). The views and conclusions contained in this document are those of the authors and should not be interpreted as necessarily representing the official policies, either expressed or implied, of the U.S. Government.

This map was created from geographic information system (GIS) files. The UGS does not guarantee accuracy or completeness of the data. Persons or agencies using these data specifically agree not to misrepresent the data, nor to imply that changes they made were approved by the Utah Geological Survey, and should indicate the data source and any modifications they make on plots, digital copies, derivative products, and in metadata.

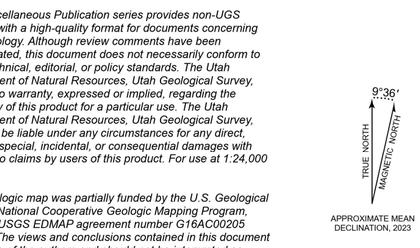

APPROXIMATE MEAN DECLINATION, 2023

SCALE 1:24,000

1 0.5 0 1 MILE

1000 0 1000 2000 3000 4000 5000 6000 7000 FEET

1 0.5 0 1 KILOMETER

CONTOUR INTERVAL 40 FEET

GEOLOGIC MAP OF THE SOUTHERN HALF OF THE RILL CREEK AND NORTHERN HALF OF THE KANE SPRINGS 7.5' QUADRANGLES

by

James P. Mauch[1] and Joel L. Pederson[2]

2023

[1]Utah State University MS thesis; now Wyoming State Geological Survey, Laramie, Wyoming
[2]Utah State University, Logan, Utah

MAP LOCATION

Base from USGS US Topo Rill Creek and Kane Springs 7.5′ Quadrangles (2017)
Shaded relief derived from USGS 10-meter NED
Projection: UTM Zone 12
Datum: NAD 1983

Fieldwork by James P. Mauch, 2015-2017
Program Manager: Stefan M. Kirby
Project Manager: Grant C. Willis (UGS)
GIS and Cartography: Lori J. Steadman, Kent D. Brown (UGS), and James P. Mauch (USU)
GIS review: Keilee A. Higgs (UGS)

Utah Geological Survey
1594 West North Temple, Suite 3110
Salt Lake City, UT 84116
(801) 537-3300
https://geology.utah.gov

https://doi.org/10.34191/MP-175DM

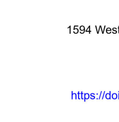

1. The Windows Section
2. Big Bend
3. Fisher Towers
4. Moab
5. Rill Creek
6. Warner Lake
7. Trough Springs Canyon
8. Kane Springs
9. Mount Tukuhnikivatz

UTAH GEOLOGICAL SURVEY
a division of
Utah Department of Natural Resources

Plate 2
Utah Geological Survey Miscellaneous Publication 175DM
Geologic Map of the Southern Half of the Rill Creek and Northern Half of the Kane Springs 7.5' Quadrangles

MAP UNITS
see booklet for descriptions of map units

- Qh — Human excavations, fill, and disturbed deposits
- Qal — Active alluvium
- Qats — Low-level alluvial sand deposits of Mill and Pack Creeks
- $Qatg_1$ — Level 1 alluvial gravel deposits of Mill and Pack Creeks
- $Qatg_{1y}$ — Level 1-younger alluvial gravel deposits of Mill and Pack Creeks
- $Qatg_{1i}$ — Level 1-intermediate alluvial gravel deposits of Mill and Pack Creeks
- $Qatg_{1o}$ — Level 1-older alluvial gravel deposits of Mill and Pack Creeks
- $Qatg_2$ — Level 2 alluvial terrace gravel deposits of Mill and Pack Creeks
- $Qatg_3$ — Level 3 alluvial terrace gravel deposits of Mill and Pack Creeks
- $Qatg_4$ — Level 4 alluvial terrace gravel deposits of Mill Creek
- $Qatg_5$ — Level 5 alluvial terrace gravel deposits of Mill Creek
- $Qatg_6$ — Level 6 alluvial terrace gravel deposits of Mill Creek
- $Qatg_7$ — Level 7 alluvial terrace gravel deposits of Mill and Pack Creeks
- $Qapg_1$ — Level 1 alluvial piedmont gravel deposits
- $Qapg_{1y}$ — Level 1-younger alluvial piedmont gravel deposits
- $Qapg_2$ — Level 2 alluvial piedmont gravel deposits
- $Qapg_3$ — Level 3 alluvial piedmont gravel deposits
- $Qapg_4$ — Level 4 alluvial piedmont gravel deposits
- $Qapg_5$ — Level 5 alluvial piedmont gravel deposits
- Qafs — Alluvial-fan sand deposits
- Qafd — Alluvial-fan debris deposits
- Qaes — Alluvial and eolian sand deposits
- Qaem — Alluvial and eolian mud and sand deposits
- Qeas — Eolian and alluvial sand deposits
- Qes — Eolian sand deposits
- Qca — Colluvial and alluvial deposits
- Qc — Colluvium
- Qcy — Active (younger) colluvium
- Qco — Older colluvium
- Qmt — Talus
- Qms — Mass movement landslide deposits
- $Qmbx_q$ — Fissure-fill collapse-breccia deposits with Quaternary gravel clasts
- $Qmbx_K$ — Fissure-fill collapse-breccia deposits with Cretaceous Mancos Shale clasts
- $Qmbx_J$ — Fissure-fill collapse-breccia deposits with Jurassic Morrison Formation clasts
- Km — Mancos Shale
- Kn — Naturita Formation
- Kbc — Burro Canyon Formation
- Jmb — Morrison Formation, Brushy Basin Member
- Jms — Morrison Formation, Salt Wash Member
- Jsmt — Morrison Formation, Tidwell Member and Summerville Formation, undifferentiated
- Jctm — Curtis Formation, Moab Member
- Jes — Entrada Sandstone, Slick Rock Member
- Jesbx — Entrada Sandstone, Slick Rock Member, brecciated
- Jcd — Carmel Formation, Dewey Bridge Member
- Jcr — Carmel Formation, Rone Bailey Member
- Jcrd — Carmel Formation, Rone Bailey and Dewey Bridge Members, undifferentiated
- Jn — Navajo Sandstone
- Jnbx — Navajo Sandstone, brecciated
- Jk — Kayenta Formation
- JTrw — Wingate Sandstone
- Trc — Chinle Formation, cross section only
- Trm — Moenkopi Formation, cross section only
- Pc — Cutler Formation, cross section only
- PPh — Honaker Trail Formation, cross section only
- PPp — Paradox Formation, cross section only

CORRELATION OF QUATERNARY UNITS

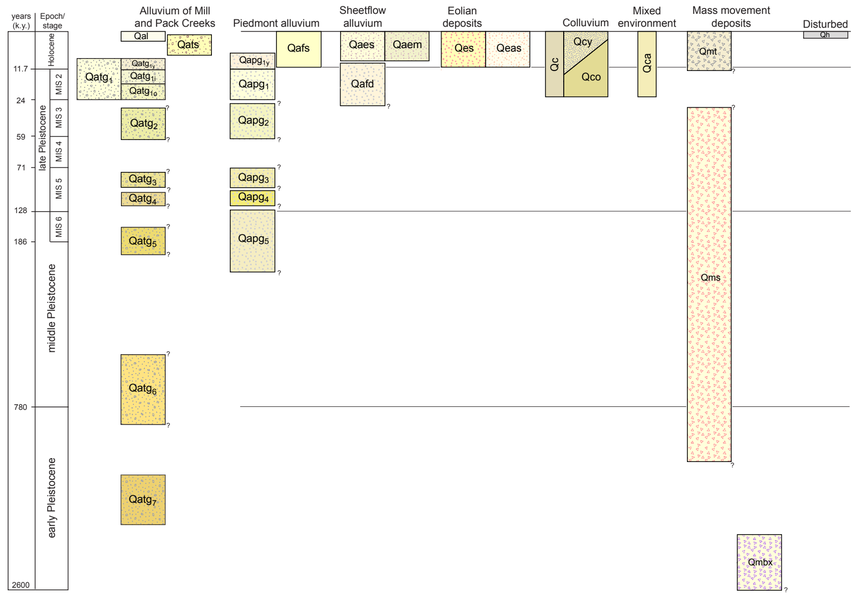

MAP SYMBOLS

- Contact: solid where well located, dashed where approximate
- Marker bed: limestone in Navajo Sandstone
- Fault, normal: solid where well located, dashed where approximate, dotted where concealed; bar and ball on downthrown side
- Fault, unknown sense of motion: solid where well located, dashed where approximate, dotted where concealed
- Anticline, upright: solid where well located, dashed where approximate, dotted where concealed
- Anticline, asymmetrical: solid where well located, dashed where approximate, dotted where concealed; double arrow on steep limb
- Monocline: solid where well located, dashed where approximate, dotted where concealed
- Syncline, upright: solid where well located, dashed where approximate, dotted where concealed
- Syncline, asymmetrical: solid where well located, dashed where approximate, dotted where concealed; double arrow on steep limb
- Strike and dip: field-measured
- Strike and dip: photogrammetric
- Joint, vertical, primary
- Joint, vertical, secondary
- Drill hole, dry
- Gravel pit
- Adit
- Arch
- Spring

CORRELATION OF BEDROCK UNITS

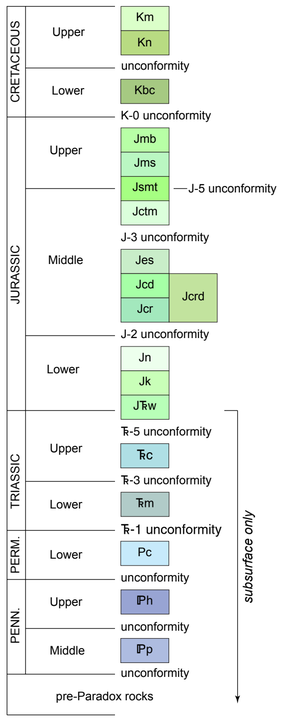

LITHOLOGIC COLUMN

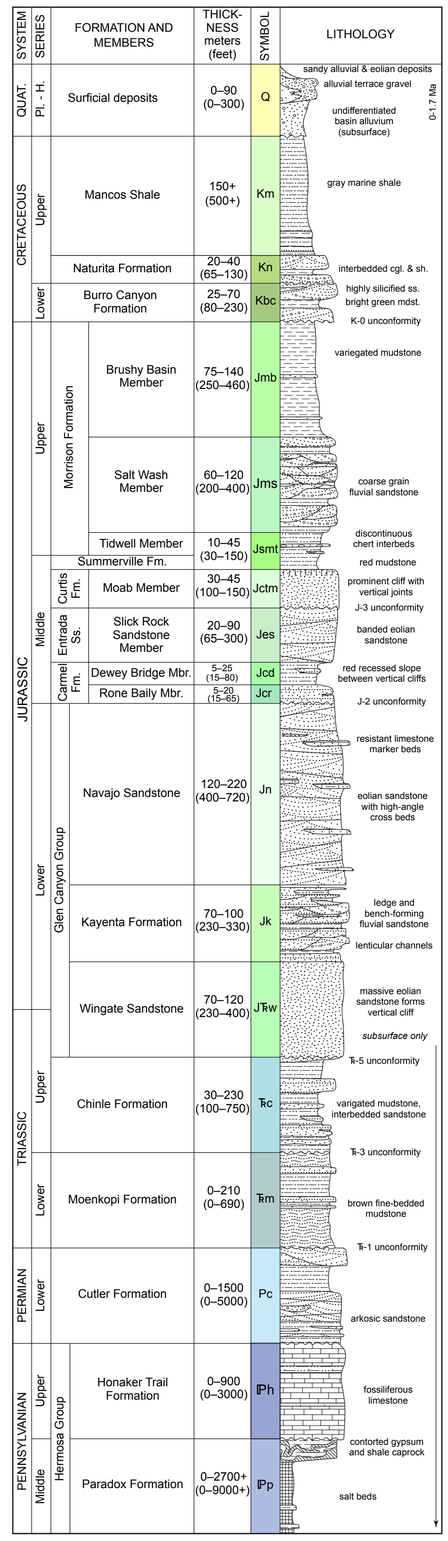

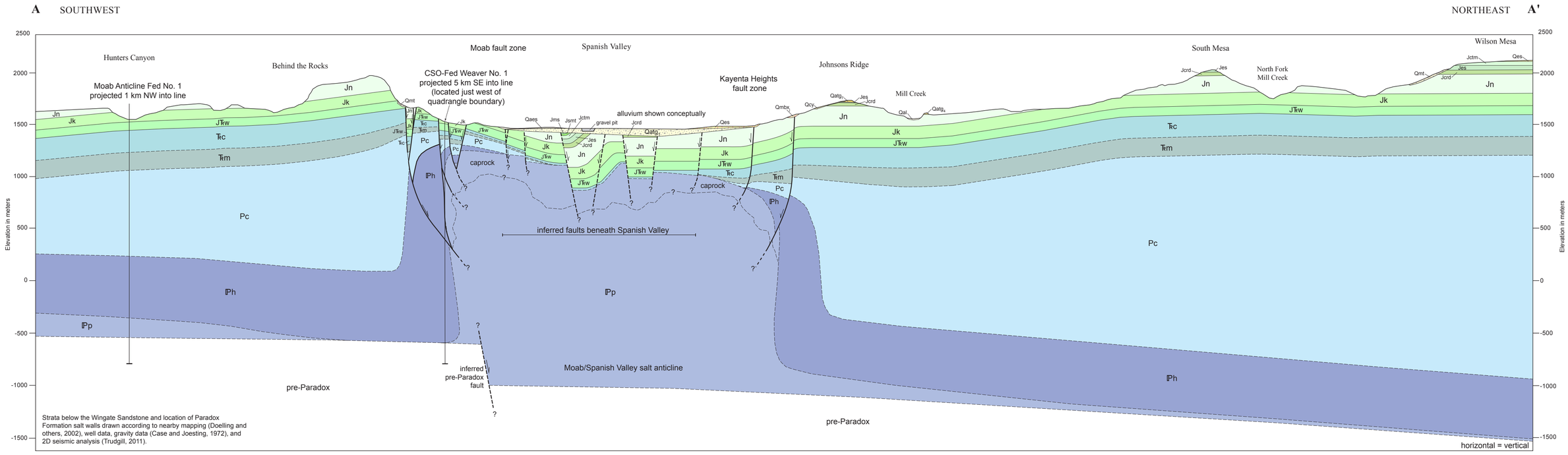

GEOLOGIC MAP OF THE SOUTHERN HALF OF THE RILL CREEK AND NORTHERN HALF OF THE KANE SPRINGS 7.5′ QUADRANGLES, GRAND AND SAN JUAN COUNTIES, UTAH

by James P. Mauch and Joel L. Pederson

MISCELLANEOUS PUBLICATION 175DM
UTAH GEOLOGICAL SURVEY
a division of
UTAH DEPARTMENT OF NATURAL RESOURCES
2023

Blank pages are intentional for printing purposes.

GEOLOGIC MAP OF THE SOUTHERN HALF OF THE RILL CREEK AND NORTHERN HALF OF THE KANE SPRINGS 7.5′ QUADRANGLES, GRAND AND SAN JUAN COUNTIES, UTAH

by James P. Mauch [1] and Joel L. Pederson [2]

[1]Utah State University MS thesis; now Wyoming State Geological Survey, Laramie, Wyoming

[2]Utah State University, Logan, Utah

Cover photo: *Southeastern Spanish Valley from the southern end of the Kayenta Heights fault zone, view is to the northwest. Knob to the right is capped by alluvial gravel deposits ($Qatg_7$).*

Suggested citation:

Mauch, J.P., and Pederson, J.L., 2023, Geologic map of the southern half of the Rill Creek and northern half of the Kane Springs 7.5′ quadrangles, Grand and San Juan Counties, Utah: Utah Geological Survey Miscellaneous Publication 175DM, 19 p., 2 plates, scale 1:24,000, https://doi.org/10.34191/MP-175DM.

MISCELLANEOUS PUBLICATION 175DM

UTAH GEOLOGICAL SURVEY

a division of

UTAH DEPARTMENT OF NATURAL RESOURCES

2023

STATE OF UTAH
Spencer J. Cox, Governor

DEPARTMENT OF NATURAL RESOURCES
Joel Ferry, Executive Director

UTAH GEOLOGICAL SURVEY
R. William Keach II, Director

PUBLICATIONS
contact
Natural Resources Map & Bookstore
1594 W. North Temple
Salt Lake City, UT 84116
telephone: 801-537-3320
toll-free: 1-888-UTAH MAP
website: utahmapstore.com
email: geostore@utah.gov

UTAH GEOLOGICAL SURVEY
contact
1594 W. North Temple, Suite 3110
Salt Lake City, UT 84116
telephone: 801-537-3300
website: geology.utah.gov

This geologic map was partially funded by the U.S. Geological Survey, National Cooperative Geologic Mapping Program, through USGS EDMAP agreement number G16AC00205 (2016). The views and conclusions contained in this document are those of the authors and should not be interpreted as necessarily representing the official policies, either expressed or implied, of the U.S. Government.

CONTENTS

FIGURES

GEOLOGIC MAP OF THE SOUTHERN HALF OF THE RILL CREEK AND NORTHERN HALF OF THE KANE SPRINGS 7.5′ QUADRANGLES, GRAND AND SAN JUAN COUNTIES, UTAH

by James P. Mauch and Joel L. Pederson

ABSTRACT

The adjoining southern half of the Rill Creek and northern half of the Kane Springs 7.5′ quadrangles are southeast of Moab, Utah. This area includes the southeastern half of the Moab-Spanish Valley salt graben and the neighboring bedrock plateaus to the southwest and northeast. Mapping of this quadrangle-sized area is part of a broader effort to understand active salt deformation and the associated landscape evolution and geologic hazards in the ancestral Paradox Basin. Strata from Late Triassic to Late Cretaceous age are exposed in the map area, and Quaternary-age units include alluvial, colluvial, eolian, mass-wasting, and fluvial terrace deposits. Graben subsidence is accommodated by systems of shallowly seated, near-vertical, gravitational faults along the margins of Spanish Valley. The two graben-margin fault zones display contrasting deformation styles and fault geometries. Ongoing Quaternary subsidence in Spanish Valley is documented in the spatial and temporal distribution of terrace deposits along Mill and Pack Creeks, which confirms previous hypotheses of active salt deformation. The hazard of active, aseismic, salt-dissolution collapse and faulting appears to be modest, with greater concern relating to attendant mass-wasting processes along the valley margins.

INTRODUCTION

The map area spans the southern half of the Rill Creek and northern half of the Kane Springs 7.5′ quadrangles, which are in eastern Utah in Grand and San Juan Counties, southeast of the city of Moab (figure 1). Much of the map area encompasses the southeastern part of the Moab-Spanish Valley salt graben, which is approximately 25 km long, 2.5 to 5.0 km wide, and trends northwest-southeast. The graben contains two alluvial valleys, Moab Valley and Spanish Valley, separated by a low topographic saddle of shallowly covered bedrock. The map area includes the entirety of Spanish Valley, and the western border intersects the bedrock saddle. The parts of the map area outside of the Moab-Spanish Valley salt graben are characterized by erosional topography typical of the Colorado Plateau, with bedrock benches and uplands bounded by escarpments and dissected by drainage networks.

The neighboring Moab 7.5′ quadrangle was mapped by Doelling and others (2002). The Kane Springs quadrangle, previously known as the Mount Peale-4 quadrangle, was mapped photogeologically by Hackman (1956). The Rill Creek quadrangle has not been previously mapped at 1:24,000 scale. The Rill Creek and Kane Springs quadrangles were included in the 1:100,000-scale map compilations by Doelling (2001, 2004). Richmond (1962) completed initial mapping and unit descriptions of the Quaternary geology in the La Sal Mountains and Spanish Valley. Harden and others (1985) proposed correlations and ages of Spanish Valley alluvial deposits based on soil carbonate concentrations, and Guerrero and others (2015) mapped graben-wide terrace gravel deposits as part of a paleoseismic study. These past workers hypothesized that subsidence of the Moab-Spanish Valley graben is active, locally rapid, and marked by deformed Quaternary alluvial deposits (Harden and others, 1985; Doelling and others, 2002; Guerrero and others, 2015).

Mapping the distribution of Quaternary deposits allows testing of previous hypotheses of active subsidence, and documenting the geometry of graben faults contributes to the understanding of the mechanics of graben collapse. Mapping is also motivated by geologic hazard concerns related to salt-dissolution faulting and subsidence around the community of Moab, which have gained attention in the wake of sinkhole openings beneath a subdivision in 2015 (Castleton and others, 2018). The city of Moab is an important economic hub for eastern Utah, relying primarily on outdoor recreation tourism, as well as mineral extraction and agriculture. A growing residential population and increased tourism have pushed development southeast into Spanish Valley, spurring the need for this geologic mapping.

Field mapping was initially conducted at 1:8,000 scale in Spanish Valley, along the graben margins, and in Mill Creek (hereafter "South Mill Creek"), North Fork Mill Creek (hereafter "North Mill Creek"), and Pack Creek. Field lines were then digitized using VrTwo photogrammetry software. The bedrock plateau southwest of Spanish Valley, the uplands between the forks of Mill Creek, and Wilson and South Mesas were initially mapped in VrTwo and subsequently field-verified. VrTwo lines were imported into ArcGIS, where the final map layout was created at 1:24,000 scale (plate 1). Units, correlations, and a cross section are on plate 2. Mapping was conducted in collaboration with the Utah Geological Survey (UGS) and partially funded by the U.S. Geological Survey EDMAP program, award G16AC00205.

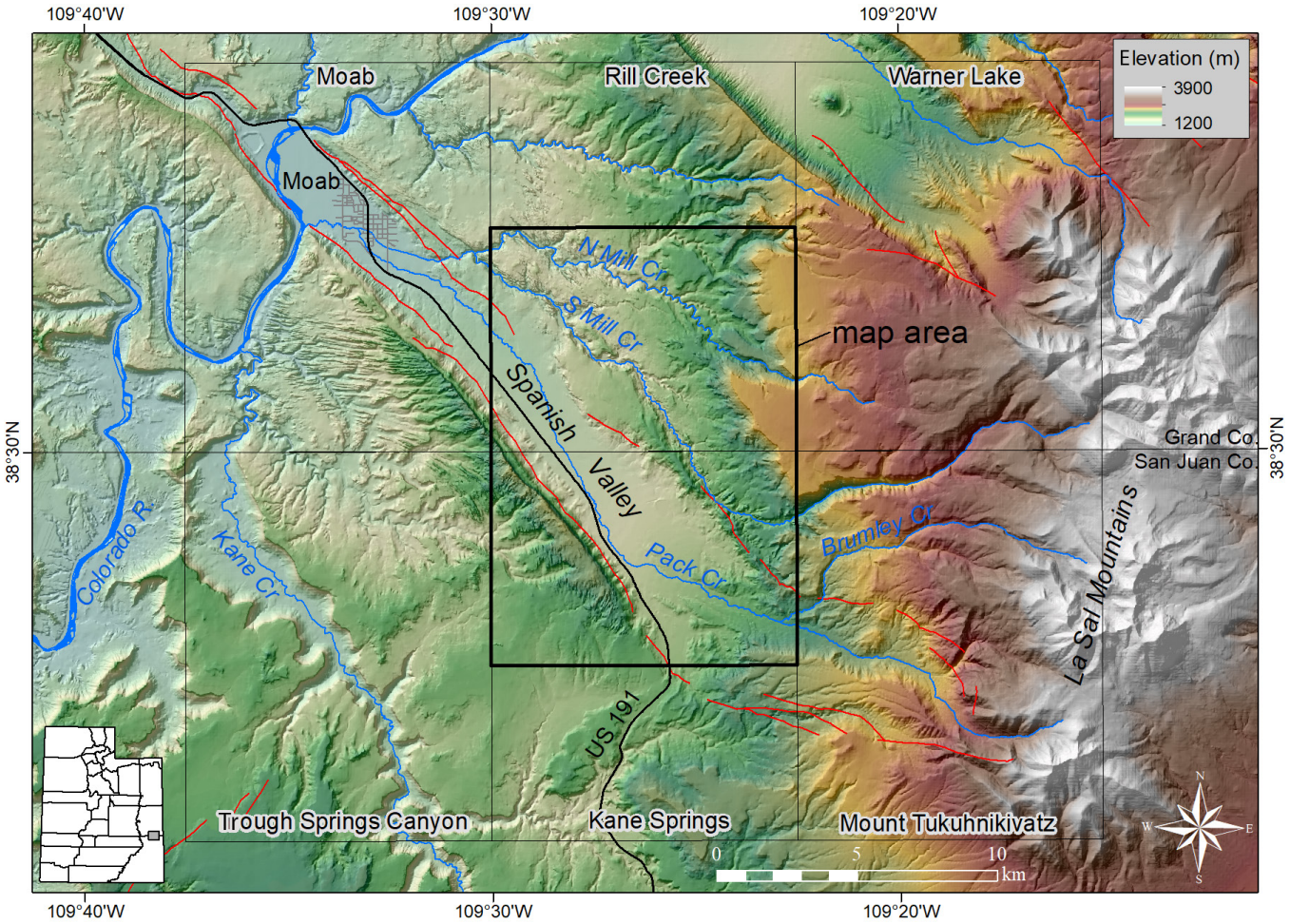

Figure 1. *The map area encompasses the southern half of the Rill Creek and the northern half of the Kane Springs 7.5' quadrangles, outlined in black. Thin black lines show neighboring 7.5' quadrangles. Red lines are Quaternary faults (U.S. Geological Survey and Utah Geological Survey, 2006). Gray rectangle on inset map shows location within the state of Utah.*

SETTING

The map area includes Spanish Valley, which is the southeastern extent of the Moab-Spanish Valley salt graben, and dissected bedrock plateaus to the northeast and southwest (figure 1). Drainages above the southwestern rim of Spanish Valley flow away from the graben, feeding Hunters Canyon, Kane Creek, and eventually the Colorado River. Northeast of Spanish Valley a lower-elevation bedrock plateau is dissected by the forks of Mill Creek. Farther east an escarpment bounds Wilson and South Mesas, which form a prominent bench anchored by resistant lithology along the eastern map boundary. Outside the map area to the east, the laccolithic La Sal Mountains form the headwaters for the three primary drainages that traverse the Rill Creek and Kane Springs quadrangles (figure 1). North and South Mill Creek are entrenched in bedrock canyons for their entire lengths in the map area, but eventually converge and enter Moab Valley orthogonally from the east. Pack Creek enters the graben axially near its southeastern terminus and flows through Spanish Valley before exiting the map area, becoming entrenched across the bedrock saddle, and joining Mill Creek in Moab Valley. Mainstem Mill Creek then joins the Colorado River just prior to the river's reentrance into a bedrock canyon after transecting Moab Valley. Mill and Pack Creeks are perennial streams but are heavily diverted for agricultural and domestic use. Elevation in the map area ranges from 1320 m along Mill Creek to 2200 m on South Mesa.

The Moab-Spanish Valley salt graben is in an area of salt deformation associated with the ancestral Paradox Basin of the central Colorado Plateau (figure 2). The Paradox Basin was a flexural-subsidence foreland basin along the southwestern flank of the basement-cored Uncompahgre Uplift that developed in middle Pennsylvanian time (Stevenson and Baars, 1986; Barbeau, 2003). The restricted basin was periodically connected with a sea to the west, and up to 2500 m of evaporites precipitated from hypersaline brines during times of basin isolation (Trudgill, 2011). These deposits compose the Paradox Formation, a sequence of 33 evaporite cycles of anhydrite, dolomite, organic-rich calcareous shale, and halite (Raup and Hite, 1992). Salt deposition spanned an area stretching roughly 325 km northwest-southeast and 150 km northeast-southwest in southeastern

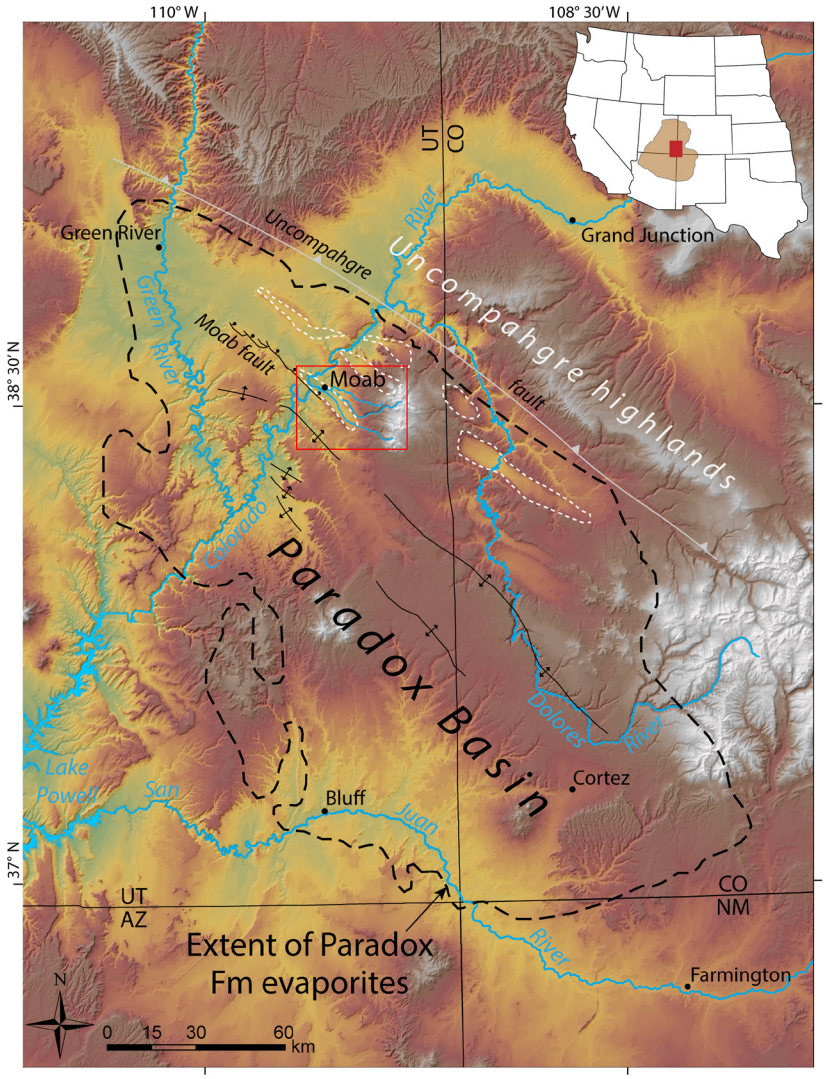

Figure 2. *Regional map of the ancestral Paradox Basin. Salt grabens are marked by white dashed lines and major folds are shown in black. Red outline shows location of figure 1; red box on index shows area of this figure. Paradox Basin evaporite facies extent (dashed black line) from Nuccio and Condon (1996), structures from Doelling (2004).*

Utah and southwestern Colorado (Barbeau, 2003) (figure 2). Deposition of the Paradox Formation ceased by the end of the Pennsylvanian, though subsidence in the Paradox Basin continued into the Late Triassic (Baars and Doelling, 1987; Doelling and others, 1988).

Ductile deformation from differential overburden pressure began during deposition as evaporites migrated laterally and rose buoyantly along pre-existing faults. The resulting diapirs and salt walls grew up to 4500 m vertically and deformed the overlying strata into a series of anticlines and synclines (Trudgill, 2011). This initial pulse of salt migration lasted into the Triassic and is responsible for lateral thickness variations, truncations, and angular unconformities in the overlying Permian and Triassic strata of the Cutler Group, Moenkopi Formation, and Chinle Formation (Doelling and others, 1988). Subsequently, salt migration diminished and was restricted to localized zones near anticline crests (Doelling and others, 1988). Salt structures were buried by Jurassic sediments and may have been dormant until reactivation from early Cenozoic (Laramide) shortening, when broad folds following the trends of the Pennsylvanian-Triassic salt anticlines and Pennsylvanian basement faults were reactivated (Doelling and others, 1988). Several northwest-striking normal faults developed in the Paleogene during or shortly after the Laramide orogeny (Olig and others, 1996; Pevear and others, 1997). This period of extensional faulting may be related to relaxation after Laramide compression (McKnight, 1940), reactivation of pre-Paradox faults (Doelling and others, 1988), or to an early phase of epeirogenic uplift of the Colorado Plateau (Parker, 1981).

The Moab fault is a 45-km-long, northwest-striking, down-to-the-northeast normal fault that extends from the Tenmile graben to the southern end of Spanish Valley (Olig and others, 1996). This fault is subdivided into three sections based

on displacement geometry and geomorphic expression. The southernmost section coincides with the Moab-Spanish Valley graben (Olig and others, 1996) and has a maximum displacement of approximately 960 m about 5 km northwest of the Colorado River, where it juxtaposes Permian and Upper Jurassic strata (Foxford and others, 1998). The Moab fault is generally interpreted to have formed in Laramide time after Mesozoic diapirism (McKnight, 1940; Doelling and others, 1988; Olig and others, 1996), though some have suggested that it reactivated older salt structures from the Triassic (Foxford and others, 1996). Estimates for last displacement on the central strand of the Moab fault range from 1.2 to 7.5 Ma based on bedrock scarp retreat rates (Olig and others, 1996) to 60 Ma based on Ar-dating of clay gouge (Solum and others, 2005). Doelling and others (2002) and Doelling (2004) inferred that the southern fault section follows the graben axis in Moab and Spanish Valleys where it is concealed beneath Quaternary deposits. This interpretation was based on well logs and seismic reflection lines in northwestern Moab Valley (Cooksley Geophysics Inc., 1995) and implies that the Moab fault is distinct from the salt-collapse deformation belts on the northeastern and southwestern graben margins (Olig and others, 1996). Alternatively, the mapping of Williams (1964) and classification by Black and others (2004) interpreted the Moab fault as bounding the southwestern margin of the Moab-Spanish Valley graben and to be spatially coincident with any salt-driven deformation. The Moab fault may have a tectonic component, but seismic reflection, aeromagnetic, and gravity data indicate that it soles in the underlying salt anticline and does not penetrate basement rocks (Woodward-Clyde Consultants, 1986; Olig and others, 1996; Trudgill, 2011).

Salt structures throughout the ancestral Paradox Basin are inferred to have been exhumed and reactivated during the late Cenozoic erosion of the Colorado Plateau (Doelling and others, 1988). It is thought that dissolution of evaporites by meteoric waters occurred preferentially along shallowly buried anticline crests, causing eight of these anticlines to collapse into salt grabens (Cater, 1970; Doelling and others, 1988). The Moab salt-cored anticline is one example, which collapsed to form the modern-day Moab-Spanish Valley salt graben. Salt dissolution left behind accumulations of insoluble gypsiferous residue atop the undissolved salts, which now forms a caprock that is exposed along both valley walls near the town of Moab, but is hypothesized to be more deeply buried beneath Spanish Valley (Baars and Doelling, 1987; Doelling and others, 2002).

Some of the few studies to document Quaternary salt deformation in the ancestral Paradox Basin were conducted around Spanish Valley. Richmond (1962) recognized that alluvial terraces along Pack Creek converge downstream, and inferred that these units were deformed by subsidence in Spanish Valley. Harden and others (1985) extended this hypothesis using soil profile analyses to correlate terrace deposits upstream of Spanish Valley to subsurface gravels and buried soils in the valley floor. They inferred that gravel deposits observed to converge, thicken, and warp into the subsurface in the middle part of Spanish Valley date to the penultimate glaciation, suggesting valley subsidence in the last 150 ky. More recently, Guerrero and others (2015) completed a paleoseismic study across a strand of the Kayenta Heights fault along the northeastern graben margin, calculating an unexpectedly high mean vertical slip rate of greater than 3 mm per year, with a most recent event post-dating 2.3 ka. These results suggest that the Moab-Spanish Valley graben is actively subsiding in the Holocene, and may be deforming more rapidly, but at less regular intervals, than tectonic faults elsewhere in the interior western U.S.

STRATIGRAPHY

Quaternary deposits in the Rill Creek and Kane Springs quadrangles are of alluvial, colluvial, eolian, and mass-movement origin (figures 3, 4, 5). Alluvial gravels in the Spanish Valley subsurface have accumulated to thicknesses of at least 90 m (Lowe and others, 2007). Seven terrace levels of alluvial gravels are present along Mill and Pack Creeks upstream of the Moab-Spanish Valley salt graben. On the bedrock plateaus and rims above Spanish Valley, fine-grained eolian sand derived from the weathering of Mesozoic sandstone is widespread and commonly remobilized by overland flow. Talus deposits are common at the base of escarpments on the margins of Spanish Valley and beneath Wilson and South Mesas to the east. Bedrock units range from the Upper Cretaceous Mancos Shale to the Jurassic-Triassic Wingate Sandstone. Middle Jurassic and older units are exposed mostly on broad red-rock benches northeast and southwest of Moab-Spanish Valley, and in fault zones and cliffs flanking the graben. Younger units are exposed in collapsed structures within the graben, most in the southern part of the map area.

DESCRIPTON OF MAP UNITS

QUATERNARY

Qh **Human excavations, fill, and disturbed deposits** (historical) – Includes gravel pits, landfills, and reservoirs.

Qal **Active alluvium** (historical and late Holocene) – Well to moderately sorted silt, sand, and gravel comprising the active channel and floodplain of large washes and perennial streams; commonly marked by tamarisk and cottonwood trees; up to 5 m thick in canyons of Mill Creek.

Qats **Low-level alluvial sand deposits of Mill and Pack Creeks** (late to middle Holocene) – Moderately sorted, coarse-grained sand to clay; forms thick alluvial

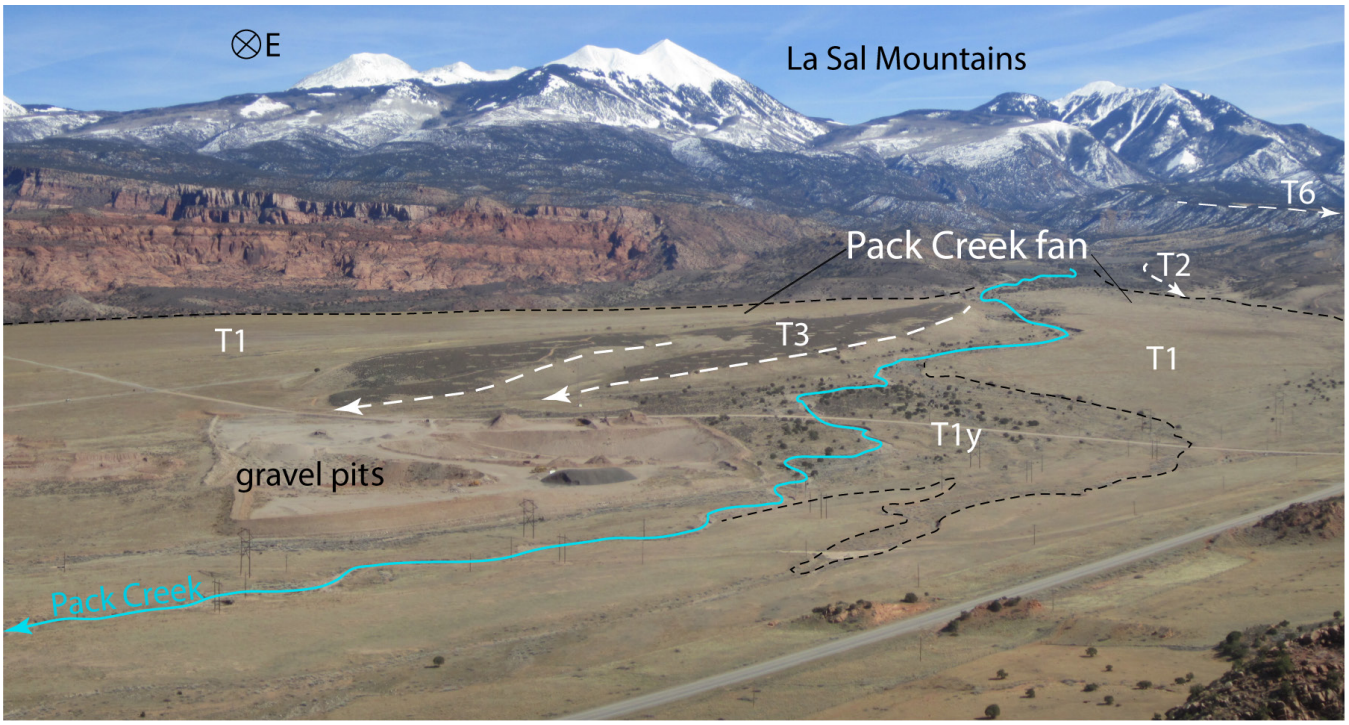

Figure 3. *Pack Creek terraces in southeastern Spanish Valley. Terraces T2 (Qatg$_2$) and T3 (Qatg$_3$) converge with the Pack Creek T1 and T1y fan (Qatg$_1$ and Qatg$_{1y}$) just up-valley from gravel pits. White dashed lines show the tops (treads) of terraces. Photo taken from 38.4698°, -109.4617° with view to the east.*

Figure 4. *Alluvial terrace deposits and upland gravels between South Mill Creek and Spanish Valley. Terrace labels T4 through T7 correspond to map units Qatg$_4$ through Qatg$_7$. View is oblique to the northwest looking downstream along South Mill Creek with the Moab-Spanish Valley graben to the left. Red star shows location of 1.43 +/- 0.42 Ma cosmogenic radionuclide burial sample of Qatg$_7$ gravel on Johnsons Ridge (Mauch, 2018). Graben faults shown conceptually. Image: Google Earth.*

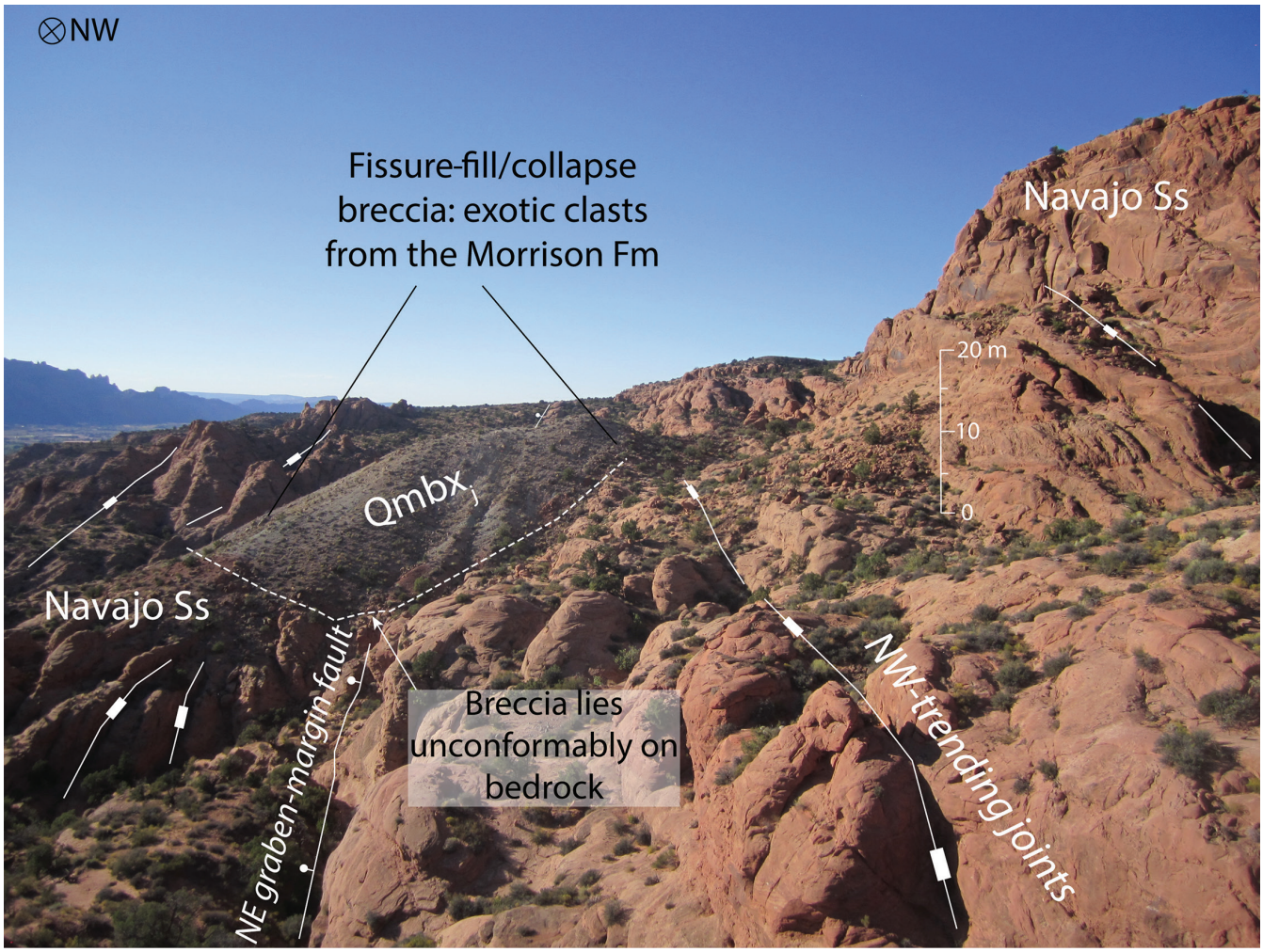

Figure 5. *Fissure-fill/collapse breccia along the northeastern graben margin below Johnsons Ridge. Deposit shown here contains unconsolidated clasts from the Morrison Formation and is mapped as* Qmbx$_j$. *Note spatial association with mapped fault and basal unconformity with bedrock. Photo taken from 38.5002°, -109.4348° with view to the northwest.*

fill overlying bedrock and terrace gravel deposits in the canyons of Mill Creek and entrenched regions of lower Pack Creek; deposits are flat-topped and commonly cut by arroyos; commonly interfingers with sand to clay slopewash from adjacent valley walls, though majority of deposit is derived from mainstem drainage; buried roots, root casts, and krotovina commonly visible in arroyo walls; 5–15 m thick.

Qatg$_1$, Qatg$_{1y}$, Qatg$_{1i}$, Qatg$_{1o}$

Level 1 (undivided, younger, intermediate, and older) alluvial gravel deposits of Mill and Pack Creeks (Holocene to late Pleistocene, OSL ages of 6–16 ka) – Moderately sorted, clast-supported, well-rounded, imbricated, pebble-cobble gravel with a matrix of fine- to medium-grained sand; pebble-cobble gravel in eastern edge of map area along Mill and Pack Creeks fines to a cobble-pebble gravel downstream in Spanish Valley; clast lithologies are primarily porphyritic trachyte from the La Sal Mountains and minor locally derived sandstone and chert; sparse sand and silt lenses up to 10 m wide; deposits underlie the floor of Spanish Valley and are incised 1–5 m by active drainages; 5–12 m thick where exposed in gravel pits, thinning to 1 m thick upstream in Mill and Pack Creeks; locally divided into Qatg$_{1y}$ (younger, ~6 ka), Qatg$_{1i}$, and Qatg$_{1o}$ (older, ~16 ka) in upper Pack Creek according to landscape position of the fill-cut treads atop the deposit.

Qatg$_2$, Qatg$_3$, Qatg$_4$, Qatg$_5$, Qatg$_6$

Levels 2–6 alluvial terrace gravel deposits of Mill and Pack Creeks (late to early Pleistocene) – Moderately sorted, clast-supported, well-rounded, imbricated, pebble gravel to boulder-cobble gravel with a matrix of fine- to medium-grained sand; sparse sand and silt lenses up to 10 m wide; clast lithologies are porphyritic trachyte from the La Sal Mountains and minor locally derived sandstone and chert; stage II-III pedogenic carbonate development. Qatg$_2$ treads

are 10–25 m above the modern channel outside of Spanish Valley and converge with the basin floor in southeastern Spanish Valley; 1–5 m thick strath terrace deposits in upstream bedrock canyons, up to 20-m-thick fill deposits downstream in Spanish Valley; OSL ages of 41–63 ka. $Qatg_3$ treads are 30–45 m above the modern channel outside of Spanish Valley and converge with the basin floor in central Spanish Valley; 2- to 8-m-thick strath terrace deposits in upstream bedrock canyons, at least 30-m-thick fill deposits downstream in Spanish Valley (base not exposed); OSL ages of 78–91 ka. $Qatg_4$ gravels are only found in South Mill Creek as 3- to 5-m-thick strath terrace deposits with treads 45–70 m above the modern channel; IRSL age of ~113 ka. $Qatg_5$ deposits are found only as incompletely preserved gravel knobs along the southwestern canyon wall of South Mill Creek; 100–115 m above the modern channel, 1–4 m thick; IRSL age of ~184 ka. $Qatg_6$ gravels are found only along the northeastern graben rim at Johnsons Up On Top Mesa, where their treads are 125–145 m above the modern channel of Mill Creek and deposits are 10–20 m thick; unknown age.

$Qatg_7$ **Level 7 alluvial terrace gravel deposits of Mill and Pack Creeks** (early Pleistocene, cosmogenic burial ages of 1.43-1.89 Ma) – Moderately to poorly sorted, clast-supported, poorly stratified, well-rounded, boulder-cobble gravel with a matrix of fine- to medium-grained sand; no preserved sand lenses; clast lithologies are primarily porphyritic trachyte from the La Sal Mountains and minor locally derived sandstone and chert; stage III pedogenic carbonate development with localized stage IV in upper 2 m beneath terrace tread; clasts on terrace treads have well-developed desert varnish; tread is 175 m above channel of South Mill Creek at Johnsons Ridge, 180 m above channel of Pack Creek at southeastern rim of Spanish Valley; deposits not present within graben; 20–30 m thick.

$Qapg_1$, $Qapg_{1y}$

Level 1 and 1-younger alluvial piedmont gravel deposits (Holocene to late Pleistocene) – Moderately to poorly sorted, clast-supported, subangular to subrounded, boulder-cobble gravel and pebble-cobble gravel with a matrix of fine- to coarse-grained sand; clast lithologies are primarily porphyritic trachyte from the La Sal Mountains and minor locally derived sandstone, chert, and paraquartzite from the Burro Canyon Formation; deposits head in piedmont drainages along valley margins and grade to or prograde onto the valley floor surface of $Qatg_1$, commonly as alluvial fans; up to 5 m thick where exposed; locally divided into $Qapg_{1y}$ (youngest) according to landscape position.

$Qapg_2$, $Qapg_3$, $Qapg_4$, $Qapg_5$

Levels 2–5 alluvial piedmont gravel deposits (Pleistocene) – Similar sedimentology and clast lithology to $Qapg_1$, except that some deposits are coarser cobble-boulder gravel; deposits originate from tributaries and valley margins and grade to or prograde onto the corresponding terrace surface ($Qatg_2$–$Qatg_5$), commonly as alluvial fans; piedmont landforms are commonly perched above the valley floor and are not always connected to a terrace deposit, especially in the southern half of the map area; up to 20 m thick where exposed.

Qafs **Alluvial-fan sand deposits** (Holocene) – Moderately to poorly sorted, coarse-grained sand to clay; forms sandy fan deposits at the mouths of ephemeral piedmont drainages and gullies; common along the southwestern margin of Spanish Valley where deposits grade to the valley floor; up to 5 m thick where exposed.

Qafd **Alluvial-fan debris deposits** (Holocene to late Pleistocene) – Poorly sorted, angular to subangular, matrix-supported boulders to sand; deposits form fans extending into thin lobes at the mouths of steep tributaries along the southwestern escarpment of Spanish Valley; up to 4 m thick.

Qaes, Qaem

Alluvial and eolian sand deposits, alluvial and eolian mud and sand deposits (Holocene) – Moderately sorted sheetwash deposits of sand and silt with minor amounts of clay outside of active channels and floodplains; horizontally laminated to low-angle cross-bedded; commonly forms a mantle on alluvial terrace and piedmont deposits; up to 3 m thick where exposed; locally mapped as Qaem where deposits are greater than 50% silt and clay in valley bottoms that head in Mancos Shale.

Qeas **Eolian and alluvial sand deposits** (Holocene) – Well to moderately sorted sheets of fine- to medium-grained sand and silt deposited by wind and reworked by sheetwash; commonly mantles alluvial terrace and piedmont deposits, forms thin cover on bedrock plateaus above the rim of Spanish Valley, fills large embayments along the foot of escarpments, and forms gently sloping surfaces between bedrock canyon walls and active washes; rarely exposed in cross section, but may display tangential cross-beds to horizontal laminations depending on intensity of alluvial reworking; distinguished from Qaes by presence of eolian cross-beds and greater topographic roughness, distinguished from Qes by lack of dune topogra-

phy; thickness varies from 1 to 2 m atop terraces and piedmonts to 12 m at the foot of escarpments.

Qes **Eolian sand deposits** (Holocene) – Well-sorted, quartz-rich, fine-grained sand and silt; forms coppice dunes in open valley bottoms and atop flat mesas, and falling dunes on the lee side of bedrock ledges along valley walls; deposits commonly mantle or are in pockets downwind of Navajo Sandstone outcrops; rarely exposed in cross section, but shows approximately 1 m tangential cross-beds; generally less than 5 m thick in sand sheets along valley bottoms and in the lee of bedrock protrusions, though a few deposits are locally 20 m thick in bedrock embayments in southeastern Spanish Valley.

Qca **Colluvial and alluvial deposits** (Holocene to late Pleistocene) – Poorly to moderately sorted, angular to subrounded boulders to sand, but most commonly pebbles, sand, and silt; deposits found at the base of hillslopes and represent colluvium or talus reworked by sheetwash; up to 3 m thick.

Qc, Qcy, Qco

Colluvium, active (younger) colluvium, older colluvium (Holocene to late Pleistocene) – Poorly sorted, clast-supported cobbles and boulders in a sandy and pebbly matrix; forms thin mantle on slopes resulting from creep and raveling; clasts are commonly reworked from other Quaternary deposits, including talus and alluvial terrace and piedmont gravels; mapped along terrace risers where deposit completely obscures and overlies internal terrace stratigraphy; typically less than 4 m thick; locally divided into Qcy (active/Holocene) and Qco (relict/late Pleistocene) based on landscape position and connectivity with colluvium source.

Qmt **Talus** (Holocene to late Pleistocene) – Poorly sorted, angular, clast-supported cobbles to 5-m-diameter boulders in a sandy matrix; clasts derived from gravity-driven mass movements and are predominantly locally sourced sandstone; deposits most commonly mantle slopes at the base of cliffs along the escarpments on the southwestern margin of Spanish Valley and below Wilson and South Mesas; can grade downslope to colluvial and mixed colluvial/alluvial deposits; up to 8 m thick.

Qms **Mass movement landslide deposits** (late to early Pleistocene) – Unconsolidated to partially intact slump blocks of the Brushy Basin Member of the Morrison Formation and the overlying Burro Canyon Formation; intact bedrock blocks exhibit inconsistent bedding orientation, and can be displaced several hundred meters down-slope; largest landslide deposit in southern quadrangle is 0.4 sq km in area with a thickness likely greater than 40 m.

$Qmbx_q$, $Qmbx_k$, $Qmbx_j$

Fissure-fill/collapse breccia deposits (Quaternary gravel, Cretaceous Mancos Shale, Jurassic Morrison Fm) (Pleistocene) – Unconsolidated, poorly sorted, angular pebbles to boulders displaced from higher stratigraphic levels that have otherwise been eroded from the local setting; downward displacement of brecciated clasts may range from 50 to 700 m, and averages 200 m; deposits form 30- to 250-m-wide conical hills or linear ridges aligned with faults, and are found exclusively on the northeastern margin of Spanish Valley; deposits sit unconformably atop in situ bedrock; interpreted as topographic inversion of erosionally resistant material derived from higher stratigraphic units of the paleo-escarpment, which fell into fissures during extension and/or dissolution episodes; exposed thickness ranges from 3 to 40 m; subdivided based on youngest lithology in deposit. $Qmbx_q$: youngest clasts are alluvial gravels from the La Sal Mountains interpreted to be displaced from higher terrace and piedmont deposits. $Qmbx_k$: youngest clasts are from the Mancos Shale. $Qmbx_j$: youngest clasts are sandstone boulders and green mudstone and siltstone granules from the Morrison Formation.

CRETACEOUS

Km **Mancos Shale** (Upper Cretaceous) – Yellow-gray to dark-gray shale; sparse horizontally laminated interbeds of sandy limestone and limy siltstone and sandstone; forms recessive slopes and valley bottoms south of Pack Creek along the southwestern axis of the Pack Creek syncline; underlying contact with Naturita Formation is gradational and intertonguing; maximum exposed thickness is 150 m.

Kn **Naturita Formation** (formerly Dakota Sandstone) (Upper Cretaceous) – Yellow-brown, tan, and yellow-gray, coarse-grained sandstone and chert-pebble conglomerate with lesser interbedded calcareous shale; interbedded coal prominent in other locations is not present in map area; forms a suite of several 3–10 m ledges and cliffs separated by shale-bearing slopes; occurs in faulted and folded foothills in southern Spanish Valley; contact with overlying Mancos Shale mapped at uppermost conglomerate bed; contact with underlying Burro Canyon Formation is irregular due to differential scouring, which leads to variable thicknesses; 20–40 m thick.

Unconformity

Kbc **Burro Canyon Formation** (Lower Cretaceous) – Dark brown sandstone and chert-pebble conglomerate with olive-green to bright green mudstone interbeds; sandstone beds are highly silicified with quartz cement and in places form paraquartzite; sandstone and conglomerate beds typically display a heavy brown-black varnish; formation can be divided into two sandstone/conglomerate ledge-forming members separated by a prominent slope-forming bright green mudstone member (not mapped separately); discontinuous limestone interbeds and chert nodules are locally present; occurs in faulted and folded foothills in southern Spanish Valley; upper contact mapped at uppermost varnished and highly silicified sandstone bed; basal contact mapped at lowermost persistent sandstone/conglomerate above the variegated slopes of the Brushy Basin Member of the Morrison Formation; thickness varies due to undulatory contact with overlying Naturita Formation, but averages 45–50 m.

Unconformity

JURASSIC

Jmb **Morrison Formation, Brushy Basin Member** (Upper Jurassic) – Variegated (gray, green, maroon, purple) mudstone and smectite clay; forms slopes and steeply convex hilltops; sparse, discontinuous interbeds of white to light red limey sandstone and siltstone; locally contains petrified wood; occurs in faulted and folded foothills in southern Spanish Valley; upper contact mapped at base of lowermost varnished sandstone/conglomerate of the Burro Canyon Formation; basal contact gradational and poorly exposed, and is mapped at the uppermost persistent sandstone lens of the Salt Wash Member; up to 140 m thick.

Jms **Morrison Formation, Salt Wash Member** (Upper Jurassic) – Brown, light tan, yellow-gray, and white, medium to coarse-grained sandstone; gray-green mudstone and siltstone interbeds form slopes between 5- to 12-m-high sandstone ledges; pebble conglomerate is common at the base of lenticular sandstone packages; several small prospects in map area target uranium mineralization in upper sandstone lens; occurs in faulted and folded foothills in southern Spanish Valley, and rim uplands northeast of the graben; basal contact poorly exposed and difficult to distinguish, but generally mapped on top of uppermost red-brown slopes of Tidwell Member and Summerville Formation; 60–120 m thick.

Jsmt **Morrison Formation, Tidwell Member and Summerville Formation, undifferentiated** (Middle-Upper Jurassic) – Rusty red to red-brown, thinly bedded mudstone and siltstone; forms slope sometimes littered with chert fragments between the sandstone cliffs of the overlying Salt Wash Member and underlying Curtis Formation; diagnostic white and red massive chert and chert nodules of the Tidwell Member are only locally present in discontinuous limestone interbeds; occurs on upland surfaces in eastern map area; less than 15 m thick along edge of graben, thickening to 45 m to the southeast; units mapped as one due to thinness and inconsistent presence of Tidwell Member chert.

J-5 unconformity between Tidwell Member and Summerville Formation

Jctm **Curtis Formation, Moab Member** (Middle Jurassic) – Pale pink, white, and gray, massive and cross-bedded, fine- to medium-grained, quartz-rich eolian sandstone; weathers to continuous cliff with conspicuous vertical joints and cross-beds; cliffs commonly appear light-brown due to varnish; forms the prominent benches of Wilson and South Mesas in eastern map area; upper contact with red-brown mudstone of the Summerville Formation is distinct; lower contact mapped at prominent color change with red/orange Entrada Sandstone and is sharp and flat; 30–45 m thick.

J-3 unconformity

Jes, Jesbx

Entrada Sandstone, Slick Rock Member (Middle Jurassic) – Banded red-orange and white, fine-grained, cross-bedded, quartz-rich eolian sandstone; cross-beds average 1 m high; forms cliffs and smooth bedrock slopes; 3- to 10-cm-diameter dissolution pockets common along cross-bed planes; locally present along the northeastern margin of Spanish Valley, pervasive beneath the rim of Wilson and South Mesas in eastern map area; unit is locally brecciated in the southeastern map area due to faulting, where it is mapped as Jesbx; lower contact in places is undulatory and intertonguing, and is mapped at the uppermost red-brown siltstone ledges of the Dewey Bridge Member of the Carmel Formation; averages 70 m thick.

Jcd **Carmel Formation, Dewey Bridge Member** (Middle Jurassic) – Red-brown siltstone and mudstone with minor fine-grained sandstone interbeds; forms a slope or recessed ledge and cliff between the smooth faces of the Entrada Sandstone and Navajo Sandstone; commonly displays undulatory bedding interpreted to represent soft-sediment deformation; distinguishable beneath the rim of Wil-

son and South Mesas in eastern map area; lower contact with Rone Bailey Member mapped at top of horizontally bedded sandstone at small recess; usually less than 20 m thick.

Jcr **Carmel Formation, Rone Bailey Member** (Middle Jurassic) – Red-brown, red-orange, and yellow-brown, horizontally bedded, fluvial sandstone and siltstone; more resistant than overlying Dewey Bridge Member, forms short cliffs; distinguishable beneath the rim of Wilson and South Mesas in eastern map area; lower contact marked by transition between planar bedding (Rone Bailey) and cross-bedding (Navajo Sandstone); 5–20 m thick.

Jcrd **Carmel Formation, Rone Bailey and Dewey Bridge Members, undifferentiated** (Middle Jurassic) – Red-brown mudstone, siltstone, and sandstone; forms slope or short bench between smooth faces of Entrada Sandstone and Navajo Sandstone; mapped where Rone Bailey and Dewey Bridge Members are indistinguishable, either from local thinning in southwestern corner of map area or from broad folding and faulting along northeastern graben margin; 8–40 m thick.

J-2 unconformity

Jn, Jnbx

Navajo Sandstone (Lower Jurassic) – Yellow-white to pale orange and pink, fine-grained, well-sorted, cross-bedded, quartz-rich, eolian sandstone; up to 6-m -high sets of tangential, high-angle cross-beds; weathers to smooth vertical cliffs or rounded domes; a 1- to 2-m-thick zone of swirly manganese oxide mineralization is common near the upper contact; forms the footwall rim along the northeastern and southwestern margins of the graben, and is the dominant lithology outside the graben; unit is locally brecciated on the northeastern margin of Spanish Valley due to faulting, where it is mapped as Jnbx; contains thin lenticular interbeds of purple to gray limestone and limy siltstone that form resistant benches and protrusions in cliff walls, mapped as marker beds; lower contact gradational and mapped at uppermost ledge of dark red sandstone of Kayenta Formation; full thickness rarely exposed in field area, 120–220 m thick.

Jk **Kayenta Formation** (Lower Jurassic) – Dark red, maroon, orange, and white, medium-grained, moderately sorted, planar to low-angle cross-bedded, fluvial sandstone with frequent red-brown siltstone interbeds; sandstone beds are lenticular and form diagnostic 2- to 5-m-high steps and ledges separated by siltstone-bearing slopes; occurs along the southwestern escarpment of Spanish Valley, near the Kayenta Heights fault zone in the northwestern map area, and in the canyons of Mill Creek; upper and lower contacts are gradational; 70–100 m thick.

JURASSIC-TRIASSIC

JTrw **Wingate Sandstone** (Lower Jurassic-Upper Triassic) – Orange, red-orange, and pale-brown, fine-grained, well-sorted, cross-bedded, quartz-rich, eolian sandstone; forms prominent vertical cliffs with blocky vertical jointing and 10- to 30-m-diameter conchoidal fractures where sheets have spalled off; cliff faces typically display dark-brown to black desert varnish; occurs along southwestern escarpment of Spanish Valley and in upper forks of Mill Creek; upper contact mapped at the top of continuous vertical cliff where exposed; basal portion and lower contact obscured by colluvium in map area; maximum exposed thickness 100 m.

TR-5 unconformity

SUBSURFACE UNITS SHOWN ON CROSS SECTION

Trc **Chinle Formation** (Upper Triassic)

TR-3 unconformity

Trm **Moenkopi Formation** (Lower Triassic)

TR-1 unconformity

Pc **Cutler Formation** (Lower Permian)

Unconformity

IPh **Honaker Trail Formation** (Upper Pennsylvanian)

Unconformity

IPp **Paradox Formation** (Middle Pennsylvanian)

STRUCTURE/NEOTECTONICS

The dominant structural features in the map area are found along the flanks of the Spanish Valley graben. Graben-bounding fault systems having a normal sense of displacement vary significantly in their geometry between the two margins. The Moab fault zone occupies the southwestern graben margin and the Kayenta Heights fault zone (KHFZ) (Doelling and others, 2002) composes the northeastern margin. Structure

outside of the graben is dominated by strata that have a 5° to 10° southwest regional dip, though there is local variation near the graben rims. Around South Mill Creek and Johnsons Up On Top, strata dip northeast at 3° to 17° in a 1- to 2-kilometer belt extending northeast from the graben. Bedrock within 5 km of both graben margins is marked by 1- to 5-meter-spaced joints, which include a primary set that is north to northwest trending and a secondary set that is northeast to north trending.

Moab Fault Zone

The southern section of the Moab fault zone (MFZ) forms the southwestern margin of the Moab-Spanish Valley graben (Black and others, 2004; U.S. Geological Survey and Utah Geological Survey, 2006). The deformation zone is typified by a series of master and subsidiary faults that accommodate strata of the Glen Canyon Group rolling over into the floor of the graben (plate 2). The zone includes both synthetic and antithetic faults and locally contains non-pervasive cataclastic deformation bands near master faults. Displacement of exposed units across the fault zone is 250 to 300 m, though total displacement including concealed fault strands in the floor of the graben is estimated at approximately 475 m (plate 2). Master faults are the farthest outboard (southwest) from the graben and form the prominent skyline escarpment southwest of Spanish Valley. Based on offset marker beds they accommodate 200 to 250 m of displacement. Master faults are broken into sub-segments up to 4 km long with an average length of 2.6 km. Sub-segment boundaries mark locations where faults step inboard or outboard, or where subsidiary faults join master faults. A prominent boundary in the map area is 1 kilometer south of the Grand/San Juan County line where the master fault steps left by 100 m. To the northwest of this segment boundary an antithetic fault bounds a narrow graben below the master fault, and a second, parallel master fault 300 m inboard of the main escarpment extends to the northwest off the quadrangle.

Subsidiary faults closer to the graben axis are shorter than master faults, averaging 0.7 km in length. Based on marker beds in the Kayenta Formation, these faults accommodate modest offsets of less than 50 m, display synthetic (down to the northeast) and antithetic (down to the southwest) sens-

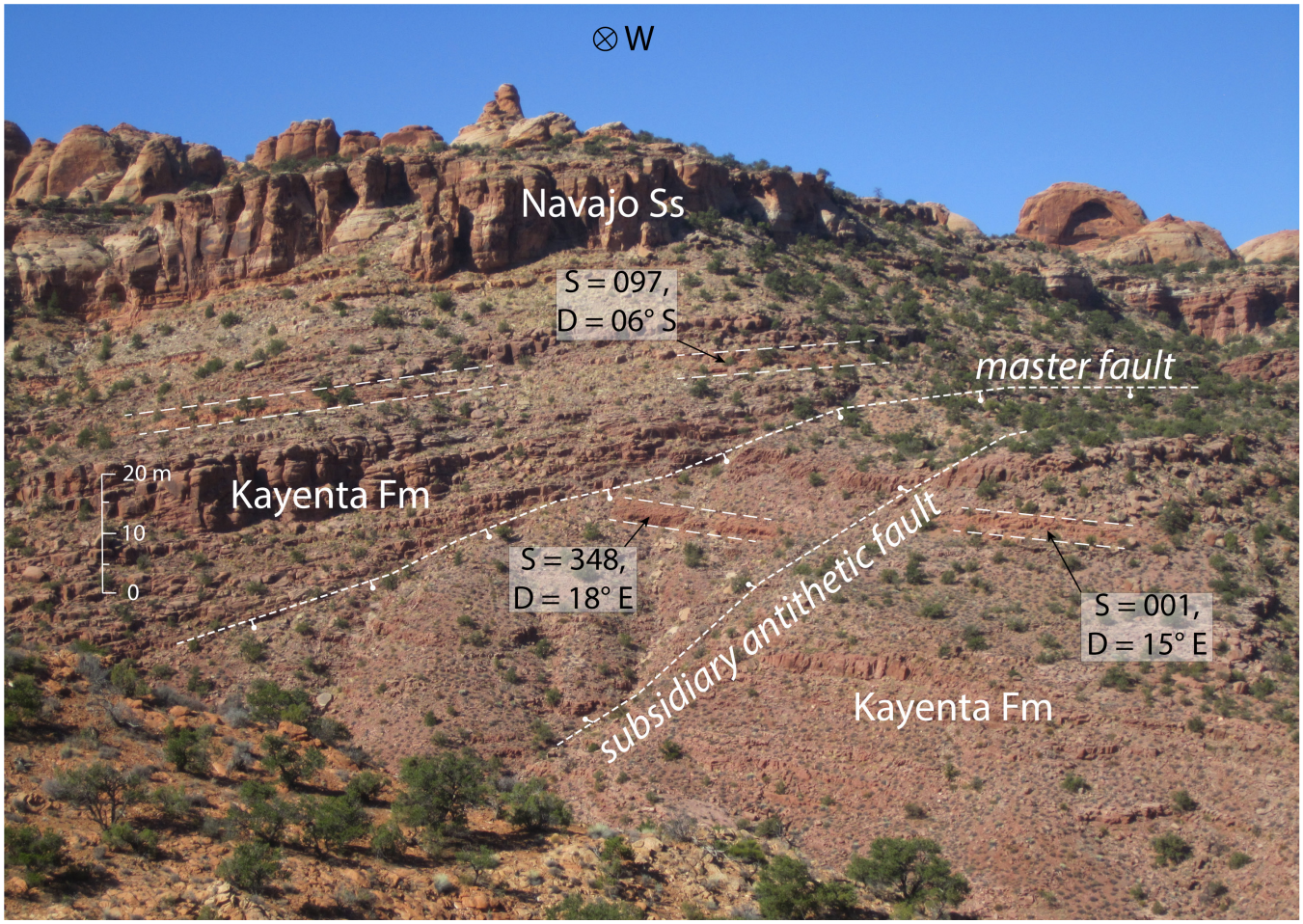

Figure 6. *Master and subsidiary faults in the Moab fault zone (MFZ). Note the change in dip of the marker bed (between white dashes) across the master fault. Photo was taken near the southeastern terminus of the MFZ where fault slip lessens and transitions into an unbroken asymmetric anticline (off the photo to the left). The master fault here displays modest throw (~20 m) compared to farther northwest along the fault zone. Photo taken from 38.4444°, -109.4383° with view to the west.*

es of slip, and separate blocks with dips that progressively steepen towards the graben (figure 6). Strata in the footwalls of the master faults dip 6° to 9° south and southwest, while bedrock hogbacks of the master fault hanging walls dip northeast at 25° to 40° (plate 1). Quaternary alluvial and eolian deposits onlap the hogbacks at the topographic floor of the graben and extend into erosional embayments along the valley margin. It is probable that additional subsidiary faults closer to the graben axis along the MFZ are concealed beneath Quaternary alluvium (plate 2). These inferred faults are required to explain the small outcrops of Cretaceous Burro Canyon Formation west and south of Kens Lake (plate 1).

The MFZ is less than 400 m wide near its southeastern termination, and widens to 1.2 km at the western edge of the map area (plate 1). The large width along the Moab-Spanish Valley graben distinguishes this southern section of the MFZ from the central and northern sections, which exhibit an approximately 10-m-wide deformation zone in exposures north of Moab (Olig and others, 1996; Foxford and others, 1998). Slip on the MFZ decreases to the southeast where the faults transition to an asymmetric anticline that drapes downward into uppermost Spanish Valley (plate 1). The MFZ continues 9.5 km off the map to the Colorado River in the northwestern direction, where caprock of the Paradox Formation is locally exposed along the base of the escarpment as a fault block (Doelling and others, 2002).

Several alternate hypotheses may account for the geometry of the Moab fault zone in Spanish Valley. They fall into end-member classes of salt-related lateral spreading and purely structural folding and faulting. A combination of these processes most likely explains the mapped geometry of the MFZ.

In the lateral spreading hypothesis, the progressive steepening of bedding towards the graben axis may record a spreading and tilting phenomenon where mapped faults are failure planes that allow mass movement blocks to slide and fall into the subsiding basin. This process has been documented in the Needles district of Canyonlands National Park and is hypothesized to result from either lateral salt flow towards areas of lower confining pressure in Cataract Canyon (Baker, 1933) or basal sliding along a tilted salt plane (Huntoon, 1982). The sliding mechanism requires a basal salt plane angled down towards the graben axis, which is not supported by seismic, gravity, or well data for Moab and Spanish Valleys (e.g., Case and Joesting, 1972; Trudgill, 2011). The lateral spreading process in the Needles fault zone has produced a deranged drainage pattern and unique fissure-fill deposits termed "swallow holes" (Geiger, 2014). The complete absence of fissure-fills in the MFZ argues against the spreading and tilting model, as extension would be expected to produce open fractures that collect overburden. Further, if opening fissures had in fact collected sediment, at least some of these deposits should be preserved in the landscape—either still in situ or as topographically inverted hills. That such fissure-fill deposits, composed of soft mudstone from the Brushy Basin Member of the Morrison Formation, are documented in the KHFZ on the other side of the graben indicates that the lack of fissure-fills in the MFZ is not simply a product of low preservation potential.

Alternatively, purely structural processes may explain some components of the MFZ geometry in Spanish Valley. The MFZ may represent a partially exhumed fault propagation fold where strata that drape into the graben are cut by subsidiary faults that connect at depth to a master fault (e.g., Sharp and others, 2000). The asymmetric anticline that marks the southeastern end of the fault zone appears to be cored by faults that have not yet breached the surface, which fits the conceptual model for a fault propagation fold (figure 6). This interpretation would imply that increased slip to the northwest along the graben margin has in fact propagated to the surface as brittle deformation, resulting in the mapped pattern of multiple faults cutting strata that roll over into the graben. However, the fault propagation fold hypothesis does not completely match observations of deformation along the MFZ. Fault propagation folds in extensional settings are typically portrayed as having subsidiary faults that converge with a master fault at depth (Sharp and others, 2000), yet the steeply dipping faults of the MFZ may not all connect at depth (plate 2) as inferred by Doelling and others (2002) in Moab Valley.

The preferred interpretation for the mapped geometry of the Moab fault zone is a combination of salt tectonic and structural processes that includes components of the lateral spread and fault propagation fold end-members. Faults in the MFZ most likely are a product of dissolution-induced subsidence rather than extension. As subsurface dissolution removes salt in the Paradox Formation, the overlying strata are displaced downward along discrete, near-vertical failure planes. The post-Paradox strata are left behind as foundered blocks amongst the insoluble caprock and are separated by synthetic and antithetic faults in the floor of the graben (plate 2). This may explain the isolated bedrock outcrops near Kens Lake (plate 1) and well data showing that alluvium in the floor of Spanish Valley is underlain by Mesozoic bedrock (Lowe and others, 2007). The graben-margin faults accommodating subsidence are interpreted to be shallowly cored in the Paradox Formation (Doelling and others, 2002; Gutiérrez, 2004), which well data indicate is no deeper than 600 m beneath the flank of Spanish Valley (Utah Division of Oil, Gas and Mining, 1973). Near the southeastern limit of the graben, salt-dissolution subsidence has not been great enough to cause brittle faulting at the surface and instead strata are folded down towards the graben floor in a hinge zone (plate 1). Faults with decreasing slip may exist beneath the surface of this fold and die out with the southeastern limit of salt dissolution. In summary, current faults in the wide, heterogeneous southern section of the Moab fault zone are interpreted as gravity-driven, shallowly rooted, and non-tectonic, which is the same as inferred by many prior workers (Cater, 1970; Doelling and

others, 1988, 2002; Olig and others, 1996; Gutiérrez, 2004; Trudgill, 2011; Guerrero and others, 2015).

Kayenta Heights Fault Zone

The Kayenta Heights fault zone (KHFZ) is characterized by linear, up to 80° dipping, down-to-the-southwest normal faults. The footwall of the fault zone is Navajo Sandstone, and the downthrown block is mostly buried beneath Quaternary alluvial deposits of Spanish Valley (plate 1). The fault zone is 1.5- to 2.0-km wide in northwestern and central Spanish Valley and narrows to 0.5 km as throw decreases to the southeast. The southeastern extent of the fault zone in the map area transitions from northwest-trending faults to a west-northwest-trending asymmetric anticline dipping steeply to the south-southwest along upper Pack Creek (plate 1). The KHFZ continues 9 km northwest to the Colorado River off the western boundary of the map (Doelling and others, 2002).

Faults of the KHFZ parallel pervasive northwest-trending joints in the Navajo Sandstone that are spaced 1 to 5 m along the graben margin. Unlike the MFZ, cataclastic deformation bands are ubiquitous throughout the KHFZ (figure 7A) and their greatest density is not always adjacent to fault strands. Bedrock along faults and fractures is commonly brecciated and bleached (figure 7B), suggesting strain localization and fluid alteration. Because cataclastic bands occur throughout the deformation zone and not just adjacent to mapped faults, they are possibly inherited from an earlier phase of deformation. Their presence along the KHFZ and near-absence along the MFZ through Spanish Valley may also record differing deformation styles between the two graben margins. However, it is also possible that this discrepancy is caused by lithologic variations between the Navajo Sandstone along the northeastern margin and the Kayenta Formation and Wingate Sandstone along the southwestern margin (plate 1), as mechanical differences between rock units can affect the density of deformation bands (Fossen and others, 2007).

The main footwall block of the KHFZ is composed of two to three parallel faults tens to hundreds of meters apart. Total displacement across the exposed width of the fault zone is approximately 200 m, though additional faults in the hanging-wall block are likely concealed beneath Quaternary alluvium (plate 2). Individual fault strands are up to 3-km long with an average length of 0.7 km, and accommodate 10 to greater than 120 m of offset. Sense of motion on all faults is down to the southwest, and there are no antithetic faults. The KHFZ includes several segment boundaries where the locus of deformation steps inboard (towards the graben) or outboard (away from the graben) or where fault planes change strike. The

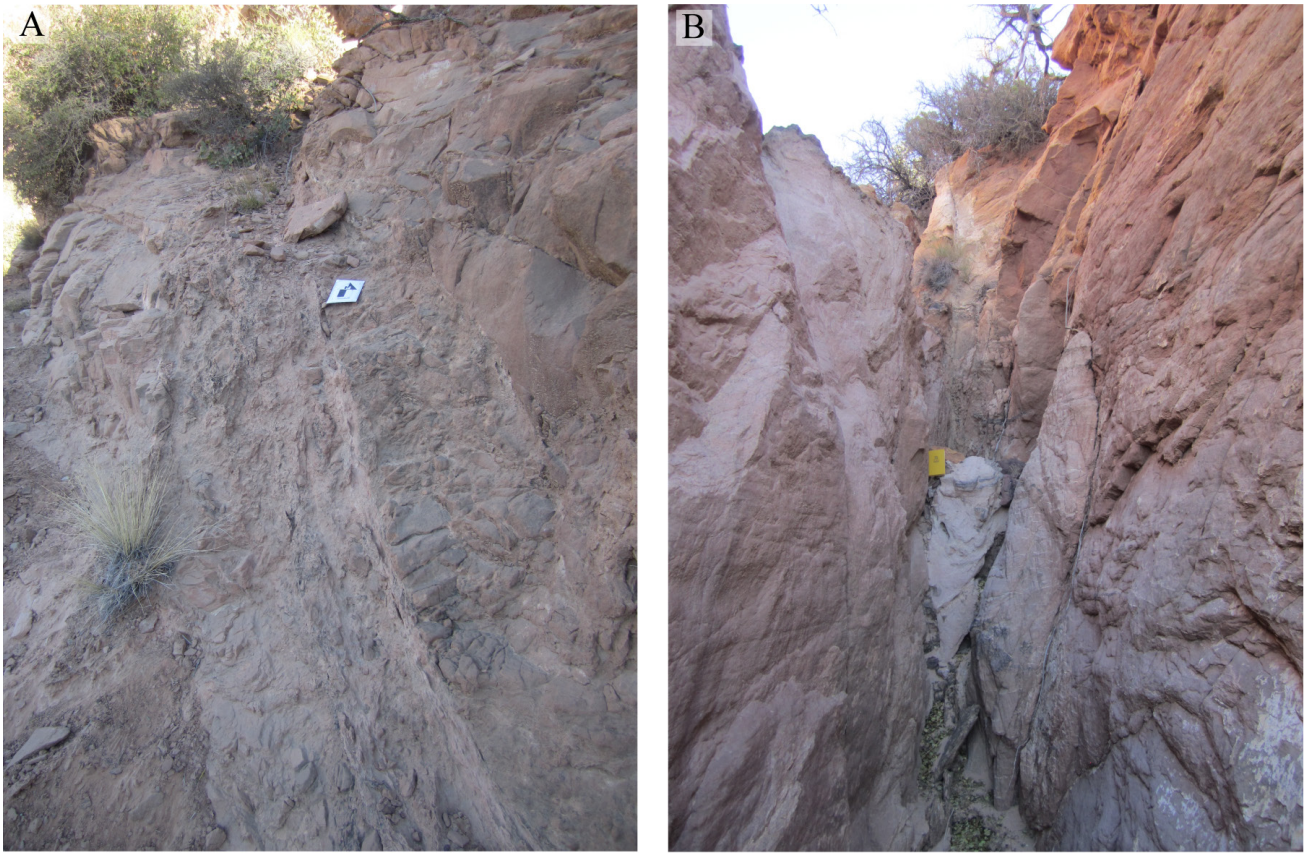

Figure 7. *Kayenta Heights fault zone deformation textures.* ***A)*** *Fault breccia and cataclastic deformation bands in the Navajo Sandstone. Location: 38.4795°, -109.4088°, view to the north.* ***B)*** *Bleaching and brecciation in the Moab Member of the Curtis Formation. Location: 38.4601°, -109.3918°, view to the southeast. Scale is 15-cm long in both images.*

boundaries are located east of Kens Lake, near the Johnsons Up On Top access road, at the northern Spanish Valley water tank (38.52, -109.47), and north of the Moab Golf Club (38.53, -109.48) where the KHFZ steps left by 1 kilometer (plate 1). The northern Spanish Valley water tank segment boundary exhibits a well-developed fault relay ramp. Where there are parallel faults along the KHFZ, the greatest displacement is along the fault closest to the graben (plate 2), suggesting that concealed faults farther inboard may accommodate even more displacement. In central Spanish Valley this farthest inboard visible fault is marked by a 1- to 2-meter-wide zone of fault breccia, and follows the straight, vertical cliff that emerges abruptly from the Quaternary deposits of the basin floor. The displacement along this escarpment must be greater than the 120 m of topographic relief, as the bedrock in the hanging wall is buried beneath eolian and alluvial deposits. In the northwestern map quadrant, a strand of the KHFZ is confined within the Navajo Sandstone in both the hanging wall and the footwall but is inferred to have only 30 to 40 m of throw (Guerrero and others, 2015). Here, an inferred fault 200- to 400-m inboard (to the southwest) juxtaposes the Salt Wash and Brushy Basin Members of the Morrison Formation against Navajo Sandstone in the footwall (plate 1), and thus produces a much greater displacement of at least 150 m.

Conical hills and linear ridges of fissure-fill breccia (Qmbx) are common in the KHFZ, but are found nowhere else in the map area—including in the MFZ. These deposits occur along or adjacent to faults and lie unconformably on in situ bedrock (figure 5). Because the basal bedrock contact is almost always visible, these deposits were not formed by sinkhole collapse in the Paradox Formation as suggested by Weir and others (1994). Instead, these features represent topographic inversion of material that fell into fissures within the Navajo Sandstone during extension. These deposits are most commonly composed of clasts from the Morrison Formation ($Qmbx_j$) displaced 150 to 250 m down-section, and overlie well-jointed but otherwise undeformed Navajo Sandstone. Fissure-fill breccias are interpreted as relict analogs to the "swallow holes" of the Needles fault zone (Geiger, 2014).

Morrison Formation clasts in fissure-fill deposits may have come from either the footwall (northeastern) or hanging-wall (southwestern) side of the KHFZ. If these clasts were derived from the footwall, fissure-fill breccias must have formed before the cliffs of the Upper Jurassic section retreated to the northeast, as the Morrison Formation is no longer present along the northeastern footwall rim of Spanish Valley. This retreat would have occurred before the deposition of the $Qatg_7$ Johnsons Ridge gravel, which is inset below exposures of the Morrison (plate 1). Alternatively, the Morrison Formation clasts in Qmbx deposits may have come from the hanging wall of the KHFZ during graben subsidence. The Morrison is exposed in the hanging wall near the western boundary of the quadrangle and is present in the asymmetric anticline at the southeastern end of the KHFZ (plate 1). The remainder of the hanging wall along the KHFZ is concealed beneath Quaternary alluvium and it is unknown if the Morrison is buried along the flanks of Spanish Valley. The hanging-wall-origin hypothesis implies that Qmbx deposits are coeval with graben subsidence, which is supported by their close spatial association with faults of the KHFZ that accommodate subsidence (plate 1). This hypothesis offers a simpler explanation for fissure-fill deposits than a footwall origin, though mapping presented here cannot confirm the origin of these unique features. Regardless, the period of fissure-fill deposition may have been distinct from the modern subsidence of the Moab-Spanish Valley graben. Although there are joints and fractures along the KHFZ today, there are no modern equivalents to the greater than 100-m-wide fissures, and no evidence for active deposition of overburden into these fissures, like there must have been during the formation of Qmbx deposits.

Implications for Graben Evolution and Subsurface Geometry

The differences in geometry between the Kayenta Heights and Moab fault zones offer insights into the evolution of the Moab-Spanish Valley salt graben. Modern deformation along both graben margins appears to be controlled by vertical gravitational collapse from the subsurface removal of dissolved salts. Mapped fault strands are high-angle (up to 80° dip), inferred to be shallowly rooted in the underlying Paradox salt wall (plate 2), and lack modern fissure-fill analogs that would imply an extensional component. However, previous workers have inferred that these modern mapped deformation belts related to Quaternary salt-dissolution subsidence are distinct from pre-collapse deformation and geometry along the crest of the Moab salt anticline (e.g., Olig and others, 1996; Doelling and others, 2002). Mapping and field observations presented here demonstrate that there may have been differences in deformation style between the Moab fault zone and what is now the Kayenta Heights fault zone prior to the ongoing period of salt-dissolution subsidence observed today. Structural relief at the base of the Navajo Sandstone between the southwestern (higher) and northeastern (lower) graben margins is 350 m (plate 2). This relief is inferred to represent the pre-collapse offset along the southern section of the Moab fault, of which the geometry and deformation style is uncertain. Furthermore, the fissure-fill breccias of the KHFZ imply a period of extension and fracture-opening that is not observed along the mapped Moab fault zone (plate 1), which may instead reflect pre-collapse or early-collapse deformation in the hanging wall of the MFZ. Collectively, these observations support the interpretation of Olig and others (1996) that Quaternary salt-dissolution subsidence accommodated along the MFZ and KHFZ is distinct in time and structural style from pre-collapse deformation along the Moab fault zone.

The relationship between modern graben subsidence and pre-collapse deformation on the Moab fault zone remains poorly understood. Prior to salt-dissolution collapse, the southern section of the Moab fault zone may have behaved much like the central section northwest of Moab, which is characterized

by a narrow (<10 m) deformation zone and the presence of cataclastic deformation bands (Olig and others, 1996; Foxford and others, 1998; Fossen and others, 2005). Because it formed along, and possibly reactivated structures related to, the initial Moab salt anticline (Doelling and others, 1988), the southern section of the Moab fault zone inevitably acted as a salt conduit and focus of collapse during the early period of salt dissolution. With the onset of Quaternary salt-dissolution subsidence, we infer that deformation along the southern section of the Moab fault changed to a wider (>1 km), more heterogenous fault zone composed of short strands that terminate at shallow depths in the Paradox Formation, while the central segment (where the adjacent salt anticline was not breached) remained relatively unchanged (Olig and others, 1996). The location of the pre-dissolution trace of the Moab fault's southern segment in relation to the Moab salt anticline is debated, as is whether evidence of this trace is still preserved. The trace has been variously mapped as following the modern-day axis of Moab and Spanish Valleys beneath the alluvial cover (Doelling and others, 2002; Doelling, 2004), coinciding with the northeastern extent of the salt wall and following the northeastern graben margin (Banbury, 2005), or following the modern southwestern escarpment of Spanish Valley (Baker, 1933; Williams, 1964; Black and others, 2004).

Two-dimensional seismic data across Moab Valley and northern Spanish Valley show a symmetrical salt wall and approximately 400 m of structural relief between Mesozoic strata on either side of the graben, but do not resolve the geometry of strata known to overlie caprock in Spanish Valley (Lowe and others, 2007; Trudgill, 2011, figure 7). Gravity data may provide additional information as to whether a pre-collapse trace of the southern segment of the Moab fault juxtaposes salt against Permian through Upper Jurassic strata beneath the alluvium of Spanish Valley (Doelling and others, 2002; Doelling, 2004). An abrupt gradient from a lower gravity anomaly to the southwest (in the footwall of the pre-dissolution Moab fault) to a higher gravity anomaly to the northeast (in the hanging wall where a thick package of denser sedimentary rocks overlies evaporites) would be the expected signal for this hypothesis, whereas a more symmetrical gravity low would argue against a major fault in the subsurface. A gravity anomaly cross section from Case and Joesting (1972) shows a symmetrical low over Moab Valley superimposed on a regional field that decreases to the northeast. The gravity survey of Hildebrand and Kucks (1983) lacks data points in and around Spanish Valley, but interpolated contours show a symmetrical gravity low. Data from the World Gravity Map (Bonvalot and others, 2012) have a 2-kilometer resolution that is too coarse to distinguish gravity differences in the bottom of Spanish Valley.

Based on the balance of this limited subsurface evidence, the cross section in plate 2 was drawn with a roughly symmetrical salt wall and without a singular, cross-cutting, pre-dissolution, Moab fault plane. Instead, the structural relief between the southwestern and northeastern graben margins is interpreted to be accommodated across a system of concealed faults that separate horst and graben blocks that are foundered within the Paradox caprock (plate 2). A faulted fold near the graben axis is inferred based on the nearest mid-valley bedrock exposures 1.8 km southeast of the cross section line, where bedding dips approximately 40° west-southwest (plate 1). A fault along the graben axis associated with the southern MFZ could possibly provide a structural control to the south- and southwest-dipping Cretaceous strata north of Pack Creek as a possible rollover anticline (plate 1). A similar rollover geometry is documented in the hanging wall of the Moab fault north of Moab Valley (Doelling and others, 2002), though the presence of this pattern in southernmost Spanish Valley is unconfirmed by subsurface evidence.

GEOLOGIC HAZARDS

Castleton and others (2018) published a comprehensive study of recognized geologic hazards in the adjacent Moab 7.5′ quadrangle, focusing primarily on Moab Valley. This geologic-hazard study used available geologic, hydrologic, soil, and geotechnical information to identify where geologic hazards may exist and where detailed, site-specific, geotechnical/geologic hazard investigations are necessary to protect health, welfare, and safety. Their study provides maps and information for 13 geologic hazards: shallow groundwater, salt tectonics-related ground deformation, flooding, landsliding, rockfall, radon gas potential, collapsible soil, expansive soil and rock, corrosive soil and rock, soluble soil and rock, piping and erosion, wind-blown sand, and shallow bedrock. Brief additional discussion of some of these hazards is provided below. Our map was requested by the Utah Geological Survey to provide the foundation of a similar study they intend to conduct in southern Moab and Spanish Valleys (Grant Willis, Utah Geological Survey, written communication, 2016).

Faulting and Seismicity

Active subsidence of the Moab-Spanish Valley salt graben is accommodated along structures that cannot be considered true tectonic faults. Interpreted as shallow-rooted features that extend only hundreds of meters into the Paradox Formation, these faults likely do not accumulate and release strain in large seismic events (Olig and others, 1996; Hylland and Mulvey, 2003; Gutiérrez, 2004) and are thus classified as Class B structures in the U.S. Quaternary Fault and Fold Database (Black and others, 2004; U.S. Geological Survey and Utah Geological Survey, 2006). This interpretation is consistent with the paleoseismic study of Guerrero and others (2015), who found that deformation along the northeastern margin of Moab Valley is both episodic and anomalously rapid (greater than 3 mm/yr), yet has a much shorter average recurrence interval (~300 years) that is more stochastic than tectonic faults. This suggests that even though rates of salt

deformation and subsidence may be as rapid as along geologically active tectonic structures, faults along the KHFZ and MFZ likely do not pose the same ground-shaking hazard.

The paleoseismic analysis of Guerrero and others (2015) and more recent mapping and geochronology along Mill Creek at the entrance to Moab Valley (Mauch, 2018) indicate that displacement across the Kayenta Heights fault zone occurred in the late Pleistocene and Holocene. Using $Qatg_4$ and $Qatg_5$ age-equivalent terrace gravels and undifferentiated alluvial deposits on either side of the KHFZ, the slip rate is constrained to approximately 500 m/my (0.5 mm/yr) since the middle to late Pleistocene (Mauch, 2018). These geochronological data for displaced late Pleistocene deposits contrast with a previous geologic hazards study of Moab Valley, which cited a lack of evidence for displacement along the graben-bounding fault zones over this time period (Hylland and Mulvey, 2003). If the southern section of the Moab fault zone along the southwestern graben margin is related to the KHFZ, the lack of displaced Quaternary units along the MFZ may reflect a period of inactivity but does not rule out future slip events. This new evidence for late Pleistocene activity along the KHFZ suggests that there is a potential surface-rupture hazard associated with graben-margin salt-dissolution faults for overlying structures and lifelines, though the conclusions of Hylland and Mulvey (2003) inferring a low ground-shaking hazard from these faults remain valid.

The primary tectonic structure in the region is the Moab fault, which pre-dates salt-dissolution subsidence of the Moab-Spanish Valley graben and extends 35 km northwest beyond the map area (Olig and others, 1996). Though its early history includes a tectonic phase (McKnight, 1940; Doelling and others, 1988), it is likely that much of its deformation has involved salt because of its position adjacent to the Moab anticline, its root in the Paradox Formation, and the regional Mesozoic and Cenozoic salt mobility documented by stratigraphic unconformities (Woodward-Clyde Consultants, 1986; Trudgill, 2011). At a minimum, it is generally agreed that the current manifestation of the Moab fault is modified by salt tectonism (e.g., Olig and others, 1996; Doelling and others, 2002; Banbury, 2005; Trudgill, 2011). The mobility and lateral flow of salt (Trudgill, 2011) has produced different structural features along strike of the Moab fault (Olig and others, 1996) which makes it challenging to infer the structural and tectonic history of the fault zone. Studies of the Moab fault ~20 km northwest of the map area concluded that the last period of major faulting was in the Paleogene and was compressional (Pevear and others, 1997; Garden and others, 2001; Solum and others, 2005). However, it is possible that the southern section of the Moab fault through Spanish Valley has had a different history, as its faulted rocks have not been dated. No microseismicity has been recognized along the Moab fault (Wong and Simon, 1981; Wong and others, 1996) and historical earthquakes greater than magnitude 4 are very rare in the Paradox Basin (Wong and Humphrey, 1989; Bowman and Arabasz, 2017). The nearest recent notable earthquakes to Spanish Valley have occurred in the Paradox Valley approximately 55 km to the southeast. Here, eight earthquakes greater than magnitude 3 have occurred since 2000, with the largest being a magnitude 4.5 in 2019 (U.S. Geological Survey, undated). However, these events are generally believed to be induced by brine deep-well injection and do not represent natural activity along shallow salt-dissolution faults (Ake and others, 2005; King and others, 2014). In summary, mapping presented here agrees with prior studies inferring that the southern section of the Moab fault zone is non-tectonic and poses a low earthquake hazard for Moab and Spanish Valleys (Olig and others, 1996; Wong and others, 1996; Hylland and Mulvey, 2003).

Rockfall and Other Mass Movement

Rockfall is a significant geologic hazard associated with salt-dissolution faulting and collapse along the margins of Spanish Valley. Rockfall is active in several other parts of the map area, such as the canyons of Mill Creek and the cliffs below Wilson and South Mesas, but poses the greatest hazard to humans in the developed parts of Spanish Valley. As the valley floor continues to subside, cliffs forming the northeastern and southwestern escarpments of Spanish Valley will continue to retreat. Rockfall is most probable along the southwestern graben margin, where topographic relief is 500 m and the MFZ footwall is pervasively jointed parallel to the escarpment free-face (Hylland and Mulvey, 2003). Extensive talus deposits of boulders from Glen Canyon Group sandstone are mapped along this valley margin (plate 1). These deposits are more widespread to the northwest, where development along U.S. Highway 191 is encroaching from Moab, and several talus cones overlie alluvial and eolian deposits along the valley floor. Rockfall in the southwestern wall of Moab and Spanish Valleys is an active hazard, as confirmed by a 2014 rockfall from the Wingate Sandstone that blocked the entrance to a railroad tunnel just north of the Colorado River with an estimated 4500 m^3 of material (Office of Environmental Management, 2015). The lesser topographic relief and scarcity of talus deposits suggests a lower likelihood of rockfall along the northeastern valley margin, though active subdivision development below the linear Navajo Sandstone escarpment between Kens Lake and the Moab Golf Club increases the probability of adverse impacts. Debris flows occur along the southwestern wall of Spanish Valley as evidenced by unsorted, boulder-rich fans (plate 1). These deposits extend less than 200 m from the base of the escarpment and as such mostly pose a hazard to immediately adjacent structures, of which there are currently none in the map area. This analysis agrees with the debris flow and rockfall-hazard map of Hylland and Mulvey (2003), which shows that the greatest hazard is along and at the base of the graben escarpments. To mitigate the societal risks of rockfall and other mass-movement events, development in Spanish Valley should occur well away from the valley walls, especially in areas where talus deposits are mapped.

Ground Subsidence

The imperceptible, large-scale subsidence occurring over the broad area of the Moab-Spanish Valley graben poses a relatively low geologic hazard. Subsidence throughout the Quaternary has averaged approximately 0.5 mm per year (Mauch, 2018). Smaller-scale, more rapid dissolution events are a concern where evaporites are near the surface. Paradox Formation caprock is exposed on the flanks of Moab Valley (Doelling and others, 2002) where dissolution produced a sinkhole collapse in 2015 (Castleton and others, 2018). There are no exposures of the Paradox Formation in Spanish Valley or anywhere else in the Rill Creek/Kane Springs map area, though the unit may be within 250 m of the surface on the northeastern edge of the MFZ (plate 2). The hazard maps of Hylland and Mulvey (2003) agree with this assessment, as they map the acute dissolution hazard from gypsiferous soil and rock as ending west of the Rill Creek quadrangle boundary (plate 1), whereas the broader-scale zone of valley subsidence (which is a low hazard) extends throughout the alluvial floor of Moab and Spanish Valleys (plate 4). Other soil and dissolution hazards recognized in Moab Valley that relate to clay-rich lithology in the Chinle and Moenkopi Formations (Doelling and others, 2002; Hylland and Mulvey, 2003) are not present in Spanish Valley, as Triassic strata are not exposed at the surface in the map area. Smectitic clay is present in the Brushy Basin Member of the Morrison Formation, which outcrops near the southeastern end of Spanish Valley (plate 1). This clay is susceptible to shrink/swell cycles when wetted and may destabilize structures built on it, of which there are only a few west of Brumley Creek. Detailed geotechnical studies are recommended in areas of potential salt- or gypsum-dissolution subsidence, clay-rich lithologies, and expansive soil and rock.

ACKNOWLEDGMENTS

This work was primarily funded by the U.S. Geological Survey EDMAP Program (award G16AC00205). Additional financial support was provided by the Utah State University (USU) Department of Geosciences, the USU Office of Research and Graduate Studies, the National Science Foundation Graduate Research Fellowship Program, EarthScope, the Geological Society of America, and the Society for Sedimentary Geology.

We thank the Utah Geological Survey (UGS) for its support and cooperation throughout the entire mapping process. Grant Willis was an invaluable advocate and provided key logistic and scientific support in ushering the project from its conception to publication. Kent Brown and Zach Anderson lent their GIS expertise at important junctures, helping transform the map into a complete digital product. Jessica Castleton and Ben Erickson shared fruitful conversations and insight about geologic hazards around Moab.

We thank Susanne Jänecke and Tammy Rittenour (USU) as well as Stephanie Carney, Michael Hylland, and Grant Willis (UGS) for their thoughtful and substantive reviews of the map and manuscript. A final thank-you is owed to former USU students Zac Williams, Rob McDermott, and Mike Turley, who provided valuable field assistance over the course of many dawn-to-dusk mapping campaigns.

REFERENCES

Ake, J., Mahrer, K., O'Connell, D., and Block, L., 2005, Deep-injection and closely monitored induced seismicity at Paradox Valley, Colorado: Bulletin of the Seismological Society of America, v. 95, no. 2, p. 664-683.

Baars, D.L., and Doelling, H.H., 1987, Moab salt-intruded anticline, east-central Utah, *in* Beus, S.S., editor, Centennial field guide, Rocky Mountain Section: Geological Society of America, v. 2, paper 61, p. 275–280.

Baker, A.A., 1933, Geology and oil possibilities of the Moab district, Grand and San Juan counties, Utah: U.S. Geological Survey Bulletin 841, 95 p., plate 1, scale 1:62,500.

Banbury, N.J., 2005, The role of salt mobility in the development of supra-salt sedimentary depocenters and structural styles: Edinburgh, University of Edinburgh, Ph.D. dissertation, 271 p.

Barbeau, D.L., 2003, A flexural model for the Paradox Basin—implications for the tectonics of the Ancestral Rocky Mountains: Basin Research, v. 15, p. 97–115.

Black, B.D., Hylland, M.D., and Hecker, S., compilers, 2004, Fault number 2476, Moab fault and deformation zones, *in* Quaternary fault and fold database of the United States: Online, https://earthquake.usgs.gov/hazards/qfaults, accessed February 2018.

Bonvalot, S., Balmino, G., Briais, A., Kuhn, M., Peyrefitte, A., Vales, N., Biancale, R., Gabalda, G., Moreaux, G. Reinquin, F., and Sarrailh, M., 2012, World Gravity Map: Bureau Gravimetrique International, scale 1:50,000,000, online, http://bgi.omp.obs-mip.fr/activities/Projects/world_gravity_map_wgm, accessed February 2018.

Bowman, S.D., and Arabasz, W.J., 2017, Utah earthquakes (1850-2016) and Quaternary faults: Utah Geological Survey Map 277, scale 1:500,000, https://doi.org/10.34191/M-277.

Case, J.E., and Joesting, H.R., 1972, Regional geophysical investigations in the central Colorado Plateau: U.S. Geological Survey Professional Paper 736, 31 p.

Castleton, J.J., Erickson, B.A., and Kleber, E.J., 2018, Geologic hazards of the Moab quadrangle, Grand County, Utah: Utah Geological Survey Special Study 162, 33 p., 13 plates, https://doi.org/10.34191/SS-162.

Cater, F.W., 1970, Geology of the salt anticline region in southwestern Colorado: U.S. Geological Survey Professional Paper 637, 80 p.

Cooksley Geophysics Inc., 1995, Reflection seismic survey of Atlas Minerals tailing site three miles northwest of Moab, Utah: Redding, California, unpublished consultant's report, 12 p.

Doelling, H.H., 2004, Geologic map of the La Sal 30′ x 60′ quadrangle, San Juan, Wayne, and Garfield Counties, Utah, and Montrose and San Miguel Counties, Colorado: Utah Geological Survey Map 205, scale 1:100,000, https://doi.org/10.34191/M-205.

Doelling, H.H., 2001, Geologic map of the Moab and eastern part of the San Rafael Desert 30′ x 60′ quadrangles, Grand and Emery Counties, Utah, and Mesa County, Colorado: Utah Geological Survey Map 180, scale 1:100,000, https://doi.org/10.34191/M-180.

Doelling, H.H., Oviatt, C.G., and Huntoon, P.W., 1988, Salt deformation in the Paradox Basin: Utah Geological and Mineral Survey Bulletin 122, 93 p., https://doi.org/10.34191/B-122.

Doelling, H.H., Ross, M.L., and Mulvey, W.E., 2002, Geologic map of the Moab 7.5′ quadrangle, Grand County, Utah: Utah Geological Survey Map 181, 34 p. pamphlet, scale 1:24,000, https://doi.org/10.34191/M-181.

Fossen, H., Johansen, T.E.S., Hesthammer, J., and Rotevatn, A., 2005, Fault interaction in porous sandstone and implications for reservoir management—examples from southern Utah: AAPG Bulletin, v. 89, no. 12, p. 1593–1606.

Fossen, H., Schultz, R.A., Shipton, Z.K., and Mair, K., 2007, Deformation bands in sandstone—a review: Journal of the Geological Society, London, v. 164, p. 755–769.

Foxford, K.A., Garden, I.R., Guscott, S.C., Burley, S.D., Lewis, J.J.M., Walsh, J.J., and Watterson, J., 1996, The field geology of the Moab fault, *in* Huffman, Jr., A.C., Lund, W.R., and Godwin, L.H., editors, Geology and resources of the Paradox Bain: Utah Geological Association Guidebook 25, p. 265–283.

Foxford, K.A., Walsh, J.J., Watterson, J., Garden, I.R., Guscott, S.C., and Burley, S.D., 1998, Structure and content of the Moab Fault Zone, Utah, USA, and its implications for fault seal prediction, *in* Jones, G., Fisher, Q.J., and Knipe, R.J., editors, Faulting, fault sealing and fluid flow in hydrocarbon reservoirs: Geological Society, London, Special Publication 147, p. 87–103.

Garden, I.R., Guscott, S.C., Burley, S.D., Foxford, K.A., Walsh, J.J., and Marshall, J., 2001, An exhumed palaeohydrocarbon migration fairway in a faulted carrier system, Entrada Sandstone of SE Utah, USA: Geofluids, v. 1, p. 195–213.

Geiger, F.L., 2014, Landscape evolution of the Needles fault zone, Utah, investigated through chronostratigraphic and terrain analysis: Logan, Utah State University, M.S. thesis, 172 p.

Guerrero, J., Bruhn, R.L., McCalpin, J.P., Gutiérrez, F., Willis, G., and Mozafari, M., 2015, Salt-dissolution faults versus tectonic faults from the case study of salt collapse in Spanish Valley, SE Utah (USA): Lithosphere, v. 7, no. 1, p. 46–58.

Gutiérrez, F., 2004, Origin of the salt valleys in the Canyonlands section of the Colorado Plateau—Evaporite-dissolution collapse versus tectonic subsidence: Geomorphology, v. 57, p. 423–435.

Hackman, R.J., 1956, Photogeologic map of the Mount Peale-4 quadrangle, San Juan County, Utah: U.S. Geological Survey Miscellaneous Geologic Investigations Map I-172, scale 1:24,000.

Harden, D.R., Biggar, N.E., and Gillam, M.L., 1985, Quaternary deposits and soils in and around Spanish Valley, Utah, *in* Weide, D.L., editor, Soils and Quaternary geology of the southwestern United States: Geological Society of America Special Paper 203, p. 43–64.

Hildebrand, T.G., and Kucks, R.P., 1983, Regional magnetic and gravity features of the Gibson Dome area and surrounding region, Paradox Basin, Utah—A preliminary report: U.S. Geological Survey Open-File Report 83–359, 34 p., 3 plates, scale 1:250,000.

Huntoon, P.W., 1982, The Meander anticline, Canyonlands, Utah—An unloading structure resulting from horizontal gliding on salt: Geological Society of America Bulletin, v. 93, no. 10, p. 941–950.

Hylland, M.D., and Mulvey, W.E., 2003, Geologic hazards of Moab-Spanish Valley, Grand County, Utah: Utah Geological Survey Special Study 107, 25 p., 4 plates, scale 1:24,000, https://doi.org/10.34191/SS-107.

King, V.M., Block, L.V., Yeck, W.L., Wood, C.K., and Derouin, S.A., 2014, Geologic structure of the Paradox Valley Region, Colorado, and relationship to seismicity induced by deep well injection: Journal of Geophysical Research Solid Earth, v. 119, p. 4955-4978.

Lowe, M., Wallace, J., Kirby, S.M., and Bishop, C.E., 2007, The hydrogeology of Moab-Spanish Valley, Grand and San Juan Counties, Utah, with emphasis on maps for water-resource management and land-use planning: Utah Geological Survey Special Study 120, 123 p. 11 plates, various scales, https://doi.org/10.34191/SS-120.

Mauch, J.P., 2018, Quaternary incision, salt tectonism, and landscape evolution of Moab-Spanish Valley, Utah: Logan, Utah State University, M.S. thesis, 252 p.

McKnight, E.T., 1940, Geology of the area between Green and Colorado Rivers, Grand and San Juan Counties, Utah: U.S. Geological Survey Bulletin 908, 147 p., plate 1, scale 1:62,500.

Nuccio, V.F., and Condon, S.M., 1996, Burial and thermal history of the Paradox Basin, Utah and Colorado, and petroleum potential of the Middle Pennsylvanian Paradox Formation, *in* Huffman, Jr., A.C., Lund, W.R., and Godwin, L.H., editors, Geology and resources of the Paradox Bain: Utah Geological Association Guidebook 25, p. 57–76.

Office of Environmental Management, 2015, Moab resumes rail shipments after rockslide: Online, https://energy.gov/em/articles/moab-resumes-rail-shipments-after-rockslide, accessed November 2017.

Olig, S.S., Fenton, C.H., McCleary, J., and Wong, I.G., 1996, The earthquake potential of the Moab fault and its relation to salt tectonics in the Paradox Basin, Utah, *in* Huffman, Jr., A.C., Lund, W.R., and Godwin, L.H., editors, Geology and resources of the Paradox Bain: Utah Geological Association Guidebook 25, p. 251–264.

Parker, J.M., 1981, Lisbon Field area, San Juan County, Utah, *in* Wiegand, D.L., editor, Geology of the Paradox Basin: Rocky Mountain Association of Geologists 1981 Field Conference Guidebook, p. 89–101.

Pevear, D.R., Vrolijk, P.J., and Longstaffe, F.J., 1997, Timing of Moab fault displacement and fluid movement integrated with burial history using radiogenic and stable isotopes, *in* Hendry, J.P., editor, Contributions to the second international conference on fluid evolution, migration and interaction in sedimentary basins and orogenic belts, Geofluids II Conference, The Queen's University of Belfast, Belfast, Northern Ireland, March 10-14, 1997: Geofluids II Extended Abstracts, p. 42–45.

Raup, O.B., and Hite, R.J., 1992, Lithology of evaporite cycles and cycle boundaries in the upper part of the Paradox Formation of the Hermosa Group of Pennsylvanian age in the Paradox Basin, Utah and Colorado: U.S. Geological Survey Bulletin 2000-B, 37 p.

Richmond, G.M., 1962, Quaternary stratigraphy of the La Sal Mountains, Utah: U.S. Geological Survey Professional Paper 324, 135 p., plate 1, scale 1:48,000.

Sharp, I.R., Gawthorpe, R.L., Underhill, J.R., and Gupta, S., 2000, Fault-propagation folding in extensional settings—examples of structural style and synrift sedimentary response from the Suez rift, Sinai, Egypt: Geological Society of America Bulletin, v. 112, no. 12, p. 1877–1899.

Solum, J.G., van der Pluijm, B.A., and Peacor, D.R., 2005, Neocrystallization, fabrics and age of clay minerals from an exposure of the Moab Fault, Utah: Journal of Structural Geology, v. 27, no. 9, p. 1563–1576.

Stevenson, G.M., and Baars, D.L., 1986, The Paradox: A pull-apart basin of Pennsylvanian age, *in* Peterson, J.A., editor, Paleotectonics and sedimentation in the Rocky Mountain Region, United States: American Association of Petroleum Geologists Memoir 41, p. 513–539.

Trudgill, B.D., 2011, Evolution of salt structures in the northern Paradox Basin—controls on evaporite deposition, salt wall growth and supra-salt stratigraphic architecture: Basin Research, v. 23, p. 208–238.

Utah Division of Oil, Gas and Mining, 1973, Well file of the Federal-Weaver No. 1 well, Grand County, Utah: Online, https://datamining.ogm.utah.gov, accessed November 2017.

U.S. Geological Survey and Utah Geological Survey, 2006, Quaternary fault and fold database for the United States: Online, https://usgs.maps.arcgis.com/apps/webappviewer/index.html?id=5a6038b3a1684561a9b0aadf88412fcf, accessed February 2018.

U.S. Geological Survey, undated, Earthquake Hazards Program, earthquake catalog: Online, https://earthquake.usgs.gov/earthquakes/search/, accessed November 2020.

Weir, G.W., Puffett, W.P., and Dodson, C.L., 1994, Solution-collapse breccia pipes of Spanish Valley, southeastern Utah: U.S. Geological Survey Open-File Report 94–417, 33 p.

Williams, P.L., 1964, Geology, structure, and uranium deposits of the Moab [1° x 2°] quadrangle, Colorado and Utah: U.S. Geological Survey Miscellaneous Investigations Map I-360, scale 1:250,000.

Wong, I.G., and Humphrey, J.R., 1989, Contemporary seismicity, faulting, and the state of stress in the Colorado Plateau: Geological Society of America Bulletin, v. 101, no. 9, p. 1127–1146.

Wong, I.G., Olig, S.S., and Bott, J.D.J., 1996, Earthquake potential and seismic hazards in the Paradox Basin, southeastern Utah, *in* Huffman, Jr., A.C., Lund, W.R., and Godwin, L.H., editors, Geology and resources of the Paradox Bain: Utah Geological Association Guidebook 25, p. 241–250.

Wong, I.G., and Simon, R.B., 1981, Low-level historical and contemporary seismicity in the Paradox Basin, Utah and its tectonic implications, *in* Wiegand, D.L., editor, Geology of the Paradox Basin: Rocky Mountain Association of Geologists 1981 Field Conference Guidebook, p. 169–185.

Woodward-Clyde Consultants, 1986, Paradox Basin draft project summary report, Chapter 1—Geology: Oakland, California, unpublished consultant's report, 5 volumes, variously paginated.